MASTERARBEIT | MASTER'S THESIS

Titel | Title

Measuring soil enzyme activity in situ through reverse microdialysis

verfasst von | submitted by

Helene Annette Peter BSc MSc

angestrebter akademischer Grad | in partial fulfilment of the requirements for the degree of

Master of Science (MSc)

Wien | Vienna, 2025

Studienkennzahl lt. Studienblatt | Degree programme code as it appears on the student record sheet:	UA 066 299
Studienrichtung lt. Studienblatt | Degree programme as it appears on the student record sheet:	Masterstudium Environmental Systems: Processes - Pollution - Solutions
Betreut von | Supervisor:	Assoz. Prof. Mag. Dr. Christina Kaiser
Mitbetreut von | Co-Supervisor:	Ksenia Guseva BSc PhD

Acknowledgement

First, I would like to thank Tina for giving me the opportunity to work on this project and for supporting my development throughout the thesis. A big thank you also to my second supervisor, Ksenia, who was always available for modelling questions and whose help greatly contributed to shaping this thesis.

Thank you to Thayer for teaching me how to use microdialysis and for always being available for questions, and to Sabrina for preparing the MUF–NAG solutions.

Thanks to the TER group in general for providing a pleasant working environment, with stimulating discussions and a friendly atmosphere.

A big thank you to my roommates, friends, my twin, and my family for supporting me so much throughout this long journey of my master's thesis and, more generally, for making my days better.

Table of Contents

General Introduction

Since the Industrial Revolution, human activities, primarily the burning of fossil fuels such as coal, oil, and natural gas, along with land-use changes such as agricultural extensification and deforestation, have caused a significant rise in atmospheric CO_2 levels from 285 to 426 ppm (NASA, 2025; Intergovernmental Panel on Climate Change (IPCC), 2022). This increase is altering the global carbon cycle and raising concerns about the future role of terrestrial ecosystems in climate regulation.

Currently, terrestrial ecosystems represent the third-largest carbon pool on Earth, storing approximately 3000 PgC. The majority of this carbon is found in soils, mainly as soil organic matter (SOC), while about 25% is stored in plant biomass (Jackson et al., 2017). Soils play a key role as carbon sinks, but this balance is fragile and may shift under ongoing climate change (Jackson et al., 2017; Cox et al., 2000).

Rising temperatures and elevated CO_2 concentrations can trigger complex and potentially opposing effects on ecosystems. Elevated CO_2 often enhances plant growth and photosynthesis, increasing root biomass, litter production, and root exudation, which in turn stimulate microbial activity (Terrer et al., 2018; Phillips et al., 2011). At the same time, warming accelerates microbial metabolism and enzymatic activity, driving faster decomposition and potentially releasing more CO_2 into the atmosphere via respiration (Alvarez et al., 2018; Stone et al., 2012). In vulnerable regions such as the Amazon, these combined effects may push ecosystems beyond critical tipping points, shifting them from carbon sinks to carbon sources (Douville et al., 2021; Cox et al., 2000).

Whether terrestrial ecosystems will continue to buffer climate change or become an additional source of atmospheric carbon remains an open question and depends on multiple factors such as land management, climate responses by microorganisms, etc. To better predict future biogeochemical feedbacks, we need a deeper understanding of how soil microorganisms, key drivers of decomposition and nutrient cycling, respond to these changing conditions (Burns, 1982).

Soil in the biogeochemical carbon cycle

To better understand the fate of carbon in soil, whether it becomes stabilized by sorption with minerals or mineralized by microbial activity, it is essential to view soil as a key component of the biogeochemical carbon cycle.

Plants absorb atmospheric CO_2 through photosynthesis and convert it into biomass. Carbon is then transferred into the soil via root exudates, decaying roots, and plant litter. For example, plants allocate approximately 1–40% of their fixed carbon to root exudates (Canarini et al., 2019).

Once in the soil, this organic material contributes to the pool of soil organic matter (SOM). Depending on the source and the nature of the SOM, microorganisms decompose and assimilate a portion of this material, releasing CO_2 back into the atmosphere through respiration. The fate of soil organic carbon (SOC) depends not only on environmental conditions such as temperature and pH, but also on the quality and origin of the carbon inputs (Zhang et al., 2020; Allison and Vitousek, 2005).

For instance, root exudates consist mainly of simple sugars and other low-molecular-weight compounds (Canarini et al., 2019), while plant litter is composed primarily of cell wall material such as cellulose, hemicellulose, and lignin (Carreiro et al., 2000). Root exudates are readily taken up by soil microbes or associate with minerals forming mineral-associated organic matter (MAOM)(Hansen et al., 2025), whereas the decomposition of more complex litter inputs requires the breakdown by specialized extracellular enzymes producted by soil microorgansims.

Extracellular Enzymes

Microbially-produced extracellular enzymes are key for soil biogeochemical cycling, as they catalyze the first step of organic matter decomposition and nutrient mineralization in soils (Carreiro et al., 2000). These enzymes are synthesized within microbial cells and secreted into the surrounding environment, where they diffuse away from the producing organism (Burns et al., 2013). Once outside the cell, they catalyze chemical reactions by binding to specific substrates and cleaving them into smaller, bioavailable products. This process can be schematically represented as:

$$\mathrm{E} + \mathrm{S} \rightleftharpoons \mathrm{ES} \longrightarrow \mathrm{E} + \mathrm{P} \tag{1}$$

where E denotes the enzyme, S the substrate, ES the enzyme–substrate complex, and P the reaction product.

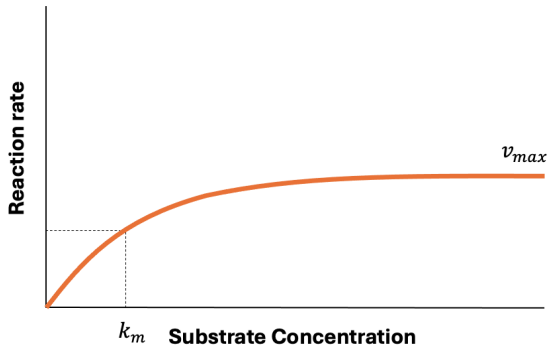

Figure 1: Simplified illustration of the Michaelis–Menten equation.

The rate of the enzymatic reaction can be described by a Michaelis–Menten (MM) kinetics, which express the reaction rate as a function of substrate concentration (Fig. 1). As substrate concentrations increase, the reaction rate rises until it saturates, reflecting that all enzyme active sites are occupied. The model is defined by two parameters: $v_{\max}$, the maximum catalytic rate, and K_m, the substrate concentration at which the reaction rate reaches half of $v_{\max}$. A low K_m indicates high enzyme–substrate affinity. Importantly, this model assumes well-mixed conditions where enzymes and substrates diffuse freely, and where substrate concentrations greatly exceed enzyme concentrations (Marangoni, 2003).

Regulation of the Extracellular Enzymes Production by microbes

In soil, extracellular enzymes are produced primarily by microorganisms. Microbes gain benefits, but also encounter costs when producing extracellular enzymes, and it is thought that they have evolved strategies to optimize enzyme production. Enzymes are composed of amino acids, and their synthesis requires substantial metabolic investment, particularly in nitrogen (N). Because extracellular enzymes are secreted, they cannot be recycled by the producing cell and the compounds are lost after secretion. An additional indirect cost of producing a public good is that reaction products may be taken up by other microorganisms, adsorbed to soil particles, or diffuse away. Microbes are therefore under strong selective pressure to develop optimized exoenzyme production strategies (Allison et al., 2011).

One regulatory strategy is the continuous secretion of small amounts of enzyme, which allows microbes to detect the presence of suitable substrates in their environment (Chróst, 1991; Allison et al., 2011). When a rise in reaction products is detected, production is upregulated. Another strategy occurs when essential nutrients are scarce and bound in complex organic matter, prompt-

ing microbes to increase enzyme production to access them (Schimel and Weintraub, 2003; Allison and Vitousek, 2005). Consequently, exoenzyme activity reflects both substrate availability and the supply of other key nutrients, particularly labile carbon and nitrogen (Allison and Vitousek, 2005; Hernández and Hobbie, 2010; Carreiro et al., 2000).

The efficiency of exoenzyme activity depends on the balance between diffusion and retention. Diffusion enables enzymes to reach otherwise inaccessible substrates, but excessive diffusion increases the risk of nutrient loss to competitors. These enzymes, often produced by specialized microbial groups, act as public goods in soils: the products of their reactions become available to surrounding microorganisms, including those that do not produce the enzymes themselves (Allison, 2005).

Soil mineral surfaces also play a crucial role, as they can immobilize enzymes, slowing their activity (Burns, 1982). Indeed, the largest enzyme pool in soil is not dissolved in water but stabilized through binding to organic matter or minerals (Burns et al., 2013).

Environmental factors such as soil pH, temperature, and moisture can further affect enzyme stability, leading to denaturation or degradation and reducing the effectiveness of enzyme production (Wallenstein and Weintraub, 2008).

Consequently, microbes must balance the metabolic costs of enzyme production with the benefits of accessing shared resources, while also mitigating losses due to diffusion, adsorption, or exploitation by other community members. Overall, extracellular enzymes are central to soil carbon cycling, and understanding their regulation and stabilization is key to predicting soil carbon sequestration in a changing climate (Burns et al., 2013).

Soil heterogeneity

A second key assumption of the Michaelis–Menten framework is that enzymes and substrates diffuse freely in a well-mixed environment. In contrast, soils are a highly complex and heterogeneous environment (Young and Crawford, 2004). The uneven distribution of minerals, water, and gases creates a network of pores with varying sizes and connectivity. These microstructures are often disconnected, which limits the movement of microorganisms and the diffusion of nutrients across niches (Tecon and Or, 2017; Nunan, 2017; Nunan et al., 2020). This structural complexity not only constrains microbial mobility but also affects the diffusion of exoenzymes within the soil matrix. Consequently, soils exhibit a wide range of microhabitats that vary in carbon and nutrient concentrations as well as microbial diversity over distances of just a few micrometres up to several millimetres (Pausch and Kuzyakov, 2011).

Zones of high microbial and nutrient abundance give rise to so-called *hot spots*, where decomposition and process rates are elevated. These dynamics vary considerably across microhabitats, influencing the cost–benefit balance for microbial exoenzyme producers in different niches. As a result, exoenzyme activity is distributed heterogeneously throughout the soil, with some pores exhibiting high activity and others showing low activity.

Root exudates and microbial hot spots

One prominent region of elevated activity is the rhizosphere, where plants release labile carbon compounds through root exudation (Canarini et al., 2019). Exudation typically occurs in pulses, especially during the daytime when photosynthesis is active (Garcia Arredondo et al., 2023). They stimulate microbial communities and can enhance nutrient availability in the rhizosphere (Kuzyakov and Blagodatskaya, 2015; Badri and Vivanco, 2009). This creates not only spatially distinct microbial hot spots in the rhizosphere but also temporal hot moments of elevated microbial activity and nutrient turnover.

Root exudates often consist of low-molecular-weight organic acids, amino acids and sugars that can be easily taken up by soil microorganisms or interact with soil minerals (Canarini et al., 2019; Badri and Vivanco, 2009). The exact nature of exudates depend on the plant and on external stressors like water content and nutrient availability. They allow the plant to control and influence the rhizosphere, cultivating beneficial microorganism and fighting pathogens. In general, the addition of labile carbon to soil often leads to a positive priming effect, characterized by accelerated decomposition of soil organic matter (SOM). In such cases, more carbon is respired than is initially introduced, resulting in a net loss of stored and stabilized carbon. One explanation is that easily available substrates activate microbial metabolism and growth, thereby increasing SOM degradation. However, labile carbon may also enhance the production of microbial exoenzymes, which remain active even after the added substrate is depleted, continuing to break down SOM (Kuzyakov, 2010).

Moreover, the nature of the root exudates plays a role, in which mechanims occurs, and which nutrient is liberated. The addition of organic acids, as charged, is expected to interact with mineral via cation exchange and so release abiotically nutirents like phosphate into the soil (Keiluweit et al., 2015). To be taken up by microbes, most organic acids have to be cleaved by very specific enzymes and requires a different metabolic pathway than sugars (Wiesenbauer et al., 2024a). Indeed, In contrast sugars are more likely to be taken up very quickly by the microorganism, and by the growth and higher enzyme production rate, stimulate the nutrient increase. For exam-

ple, following exudation, microbes may become nitrogen-limited and respond by producing more nitrogen-acquiring exoenzymes, indirectly supporting plant nutrient (Kuzyakov, 2002; Schimel and Weintraub, 2003)

Chitinase Activity and N availability

Chitin is one of the most abundant polysaccharides in soil and is composed of N-acetyl-D-glucosamine monomers linked via β-1,4-glycosidic bonds. It represents one of the dominant nitrogen (N) sources for soil organisms (Kögel-Knabner, 2002). The exoskeletons of fungi and arthropods are the main sources of chitin polymers in soil. Degradation of chitin is primarily catalyzed by hydrolytic enzymes such as chitinases, which are produced by several soil microorganisms, particularly fungi (Gooday, 1990; Thakur et al., 2023).

The production of chitinase by fungi is mainly regulated by the availability of carbon and nitrogen in the soil (Olander and Vitousek, 2000) and contributes to the recycling of fungal necromass. Specifically, the presence of chitin has been shown to strongly enhance chitinase activity (Hernández and Hobbie, 2010). This supports the hypothesis that enzyme production is upregulated in response to substrate availability, or alternatively, that the microbial community shifts toward a more fungal-dominated composition under such conditions (Hernández and Hobbie, 2010).

Measuring enzyme activity in soil

The first measurements of enzyme activity in soils were conducted between 1905 and 1910, focusing on catalase and peroxidase activity. In such assays, a saturating concentration of an artificial substrate is added to soil suspensions to quantify the *potential* activity of soil enzymes under standardized laboratory conditions.

A widely used technique for measuring EEA is the fluorometric 4-methylumbelliferyl (MUF)-based assay. In this method, soil is homogenized and transformed into a soil slurry by sieving, mixing with water, and ultrasonic treatment (Saiya-Cork et al., 2002). This leads to the release of extracellular enzymes from soil particles (Saiya-Cork et al., 2002). The MUF-labelled substrate (e.g. MUF-phosphate) is then added to the slurry. When the target enzymes cleave the substrate, the fluorescent molecule MUF is released, and its fluorescence intensity is measured over time in a 96-well microplate reader (Kremer, 1994; Saiya-Cork et al., 2002).

The fluorescence signal is proportional to enzyme activity, allowing researchers to estimate potential enzyme activity rates. This approach also provides activity parameters such as $v_{\max}$ and K_m. In natural habitats such as soil, where multiple enzymes can typically cleave a specific substrate, the

measured activity reflects the collective action of a group of enzymes rather than a single enzyme (Burns et al., 2013). Decomposition in soils is largely driven by hydrolytic and oxidative enzymes that cleave key structural polymers, including cellulose, hemicellulose, and chitin (Allison et al., 2007). To classify the vast diversity of soil enzymes, they are often grouped according to the biogeochemical cycles in which they participate, such as sulfur, phosphorus, or nitrogen cycling (Dick, 2011). The functional benefits of these enzymes vary widely depending on environmental factors, including temperature, moisture, and soil structure, which influence enzyme stability and substrate accessibility.

Although these assays have been instrumental for understanding soil enzymology, they also have limitations. The homogenization step disrupts the soil's physical structure and the natural spatial distribution of microorganisms and substrates, making these measurements representative of *average* rather than *in situ* enzyme activity (Buckley et al., 2019; Wallenstein and Weintraub, 2008).

A new method for measuring enzyme activity: Reverse microdialysis

The **key motivation of this thesis** is to develop and validate a method that allows direct and minimally invasive measurement of extracellular enzyme activity within intact soil cores, preserving the natural spatial distribution of enzymes, microbes, and substrates. Gaining insight into local extracellular enzyme activity (EEA) in intact soil cores enables the investigation of small-scale biochemical reactions and processes. As, maintaining the intact soil structure preserves the natural spatial distribution of resources and decomposers, which strongly influences microbial access to substrates and therefore affects microbial activity and decomposition processes, factors often overlooked in other approaches (Nunan et al., 2020).

The method introduced in this study to investigate in-situ EEA is based on *reverse microdialysis*. This passive sampling technique relies on diffusion driven by concentration gradients between a small semi-permeable membrane and the surrounding soil. This allows the introduction and retrieval of dissolved substances around the probe with minimal disturbance(Miró and Frenzel, 2005). This approach has been successfully applied to simulate root exudation by introducing readily available carbon compounds and subsequently collecting metabolites (König et al., 2022; Wiesenbauer et al., 2024b). In this study, we complemented experimental work establishing this new method with a NetLogo model designed to explore the dynamics and fluxes of substrates and fluorogenic compounds within the microdialysis system.

Manuscript

Introduction

Soil, one of Earth's largest carbon sinks, hosts diverse microbial communities that play a central role in decomposing organic matter and influencing carbon cycling. A key mechanism by which microbes mediate these processes is the production of extracellular enzymes, which catalyze the initial and often rate-limiting steps of organic matter degradation and nutrient mineralization (Carreiro et al., 2000). By breaking down complex organic matter derived from plant and microbial debris, these enzymes release bioavailable nutrients for surrounding microorganisms and plants (Burns et al., 2013; Gessner et al., 2010). Extracellular enzymes therefore play a central role in regulating soil carbon fluxes, and improving our understanding of their activity is crucial for predicting carbon sequestration under changing climatic conditions (Burns et al., 2013).

After secretion, exoenzymes are a public good, as their products are available to other microorganisms in close proximity (Allison, 2005). Since enzymes are amino-acid based and costly to synthesize, particularly in nitrogen (N), microorganisms have evolved strategies to optimize their extracellular enzyme production (Allison et al., 2011). It has been hypothesised that microbes initially secrete low levels of extracellular enzymes to detect the presence of specific substrates in their environment (Chróst, 1991; Allison et al., 2011). If the concentration of the enzymatic product increases, this indicates to the microbes that the corresponding substrate is available. Another regulation mechanism occurs when the target nutrient is scarce and bound within complex organic matter. In this case, microbes might upregulate enzyme production to access it (Schimel and Weintraub, 2003; Allison and Vitousek, 2005). In addition, the synthesis and excretion of enzymes, which are composed of amino acids, induce substantial carbon (C), nitrogen (N), and energy costs. Therefore, exoenzyme activity depends not only on the presence of the substrate but also on the availability of other key nutrients, particularly labile forms of C and N (Allison and

Vitousek, 2005; Hernández and Hobbie, 2010; Carreiro et al., 2000).

Another aspect that limits our understanding of organic matter decomposition is the heterogeneity of soils. Soil is a highly complex and heterogeneous environment (Young and Crawford, 2004), with uneven distribution of minerals, water, and gases creates a network of pores with varying sizes and connectivity. These microstructures are often disconnected, limiting the movement of microorganisms and the diffusion of nutrients across soil microsites (Tecon and Or, 2017; Nunan, 2017; Nunan et al., 2020). This structural complexity not only constrains microbial mobility but also affects the diffusion of exoenzymes within the soil matrix. The efficiency of exoenzyme activity depends on the balance between diffusion and retention. While diffusion allows enzymes to reach substrates that would otherwise be out of reach, too much diffusion can cause them to spread too far from the microbes that produced them, making it harder to recover nutrients. Additionally, mineral surfaces in the soil regulate exoenzyme availability. These surfaces can bind enzymes, rendering them immobilized and slowing their activity (Burns, 1982). These dynamics vary significantly across microhabitats, altering the cost-benefit balance for microbial producers in different soil microsites. Microenvironments differ in both microbial community composition and nutrient availability. As a result, this fine-scale heterogeneity can have a stronger influence on the effectiveness of extracellular enzyme production and on microbial processes than global-scale environmental factors (Tecon and Or, 2017; Nunan, 2017; Nunan et al., 2020; Schlüter et al., 2020).

Although soils are inherently heterogeneous, most studies of enzyme activity have been conducted under homogenized conditions. Conventional assays involve homogenizing, diluting, buffering the soil and ultrasonication, an invasive procedure that removes spatial heterogeneity. This can lead to new predation, competition for substrate, new mineral associations, and therefore to a community shift (Wallenstein and Weintraub, 2008). It remains unclear whether spatial variation in extracellular enzyme activity (EEA) is primarily driven by microbial regulation or by shifts in community composition, as different microbes produce different enzymes at different rates. Also, the largest pool of enzymes in soil is not dissolved in water but stabilized through binding to organic matter or minerals (Burns, 1982). These bonds are disrupted during the ultrasonication usually applied in conventional soil EEA assays (Olander and Vitousek, 2000; Burns et al., 2013). In conclusion, when using conventional homogenization-based methods, the measured EEA rate represents a bulk average across the entire soil core. Moreover, this value is biased because it measures not only the potential activity of dissolved enzymes or the enzymes that would be active under in-situ conditions, but also the activity of enzymes released due to ultrasonication (Buckley et al., 2019; Wallenstein and Weintraub, 2008; Burns et al., 2013).

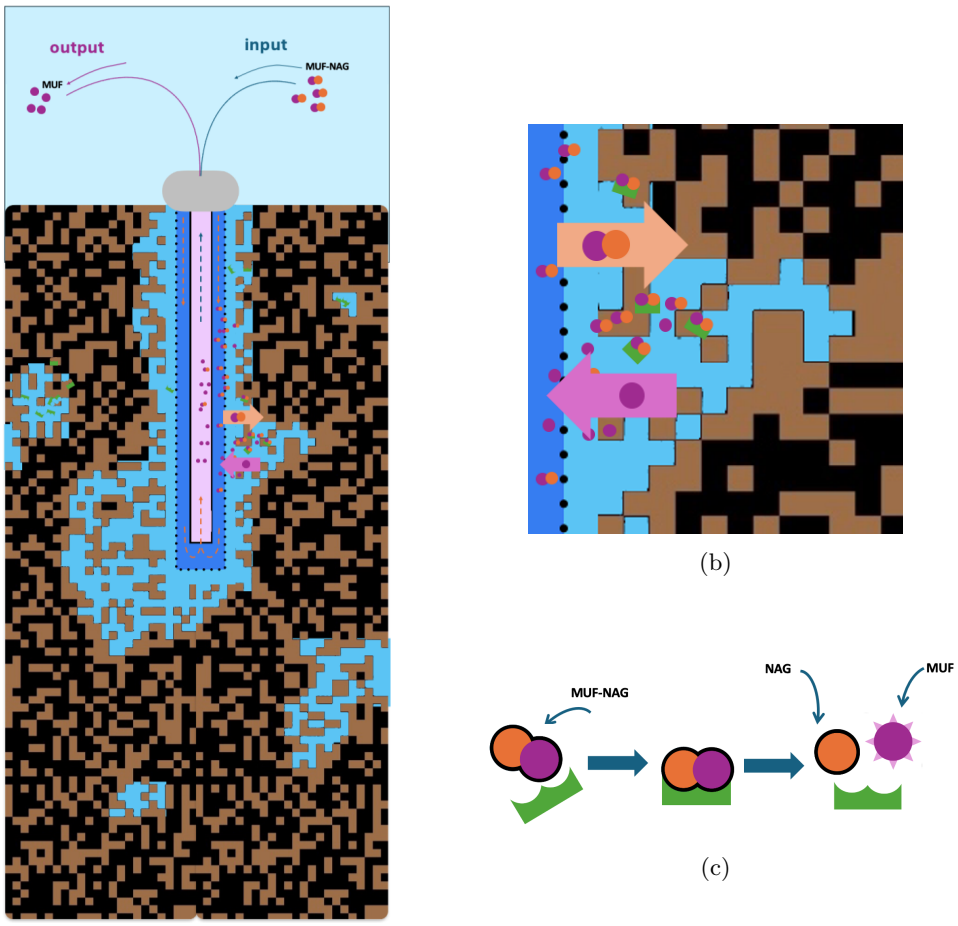

(a) (b) (c)

Figure 2: (a) Schematic illustration of the microdialysis system inserted into a soil core, showing the underlying principle of the method. The microdialysis probe is positioned in an intact soil core, where soil particles are shown in brown, soil pores in black, and water in blue. The perfusate flows from the input, through the probe tip, to the output. The semipermeable membrane enables diffusion of MUF-substrate outward (orange arrow) and MUF inward (purple arrow). Enzymes (green) are dissolved in the soil water and form complexes with the MUF-substrate. (b) Zoom-in of panel (a), highlighting the interface between soil and probe and the presence of enzymes. (c) Schematic representation of the MUF-NAG enzymatic reaction.

In this study, we introduce a new method based on microdialysis to enable *in situ* measurement of extracellular enzyme activity (EEA) in undisturbed soils. Microdialysis is a passive sampling technique that consists of a tubing system and a 1 cm probe tip with a semi-permeable membrane (see Figure 2). Concentration gradients drive diffusion between the semi-permeable membrane and the surrounding soil. Reverse microdialysis, in particular, allows the localized introduction and collection of dissolved substances with minimal disturbance to the soil matrix and microbial communities (Miró and Frenzel, 2005).

This approach has previously been used to simulate root exudation by introducing readily available carbon compounds and subsequently collecting the resulting metabolites (König et al., 2022;

Wiesenbauer et al., 2024b). Moreover, reverse microdialysis has been successfully applied to directly extract exoenzymes from soil, enabling the use of the dialysate solution for activity measurements instead of homogenized soil slurries (Buckley et al., 2019). Overall, microdialysis permits highly localized introduction and recovery of compounds while preserving soil structure, microbial communities, and functional interactions.

Rather than extracting exoenzymes from soil to measure their activity outside their natural environment, as (Buckley et al., 2019) did, we aim to assess enzyme activities directly within their natural soil habitat. To achieve this, we utilized the unique capability of microdialysis to collect and release substances from and to the soil solution via diffusion, and integrated it with an adapted version of a widely used conventional enzyme measurement assay. In both the conventional and our new microdialysis approach, a synthetic MUF-substrate is introduced, which is cleaved by soil enzymes to release the fluorescent product 4-methylumbelliferone (MUF) that can be quantified using a fluorometer (Kremer, 1994; Saiya-Cork et al., 2002). Enzyme assays using artificial substrates are typically performed under saturating substrate concentrations to estimate 'potential' activity, independent of substrate availability. Enzymatic reactions generally follow Michaelis–Menten kinetics: at low substrate concentrations, reaction rates increase linearly, but approach a maximum once all enzyme sites are saturated. By measuring reaction rates across a range of substrate concentrations, kinetic parameters such as $V_{\max}$ and the substrate concentration at which saturation occurs can be estimated.

In the microdialysis setup, the probe is inserted into an intact soil core and perfused with MUF-substrate solution. At the probe tip, the substrate diffuses out into the surrounding soil, where it can be cleaved by extracellular enzymes. The released MUF then diffuses back into the probe, where it is collected and quantified (Fig. 2). As in the conventional slurry assay, the increase in MUF concentration in the collected solution can be related to the EEA rate. One challenge, however, is that the substrate solution itself contains free MUF. In slurry assays, this is corrected by measuring fluorescence before and after incubation to obtain the net increase in MUF per unit soil mass.

In contrast to the conventional method, microdialysis reflects multiple interacting processes beyond enzyme reactions: (i) transport of MUF–substrate through the probe, (ii) diffusion across the membrane, (iii) diffusion in the soil matrix, (iv) enzymatic cleavage, (v) diffusion of MUF back to the probe, and (vi) its passage into the probe (see Fig. 2). The signal integrates all these steps, making it difficult to isolate enzyme activity, especially since several processes remain unknown or unmeasurable.

Therefore, quantifying EEA via microdialysis introduces several technical challenges:

1. **Diffusion volume.** Unlike the fixed geometry of a 96-well plate, a soil core has no clear boundaries, making it difficult to know how much surrounding soil contributes to the measured activity or how far MUF–NAG and MUF diffuse. Both compounds may spread away from the probe or become immobilized by abiotic or biotic processes. These dynamics depend strongly on soil structure and water content, leading to a central question: **How does diffusion volume shape the measurement, and how much of the added MUF can actually be recovered?**

2. **Calibration.** Interpreting dialysate MUF is complicated by the presence of residual MUF in the MUF–substrate solution. In slurry assays, this can be corrected by simple subtraction, but in microdialysis the situation is different because flux between the probe and the soil changes over time. Moreover, the dialysate represents perfusate collected over an interval, so it reflects the accumulated MUF rather than an instantaneous value. Accurate correction therefore requires accounting for these dynamics instead of relying on a simple baseline subtraction. **Can we correct for MUF in the perfusate, and can we still reproduce a Michaelis–Menten curve with microdialysis?**

3. **Sensitivity to treatments.** Additions of nutrients or carbon sources such as acetate or NAG are expected to locally alter extracellular enzyme activity. **Can microdialysis detect significant changes in *in situ* activity.**

To address these challenges and establish this new approach, we conducted a series of experiments and developed a NetLogo model to simulate substrate diffusion under different outside conditions, as in an aqueous solution and in soil cores. Together, the experimental and modeling approaches provide a detailed understanding of MUF–NAG and MUF dynamics in soil and enable accurate comparisons of extracellular enzyme activity under controlled conditions.

Methods

2.1 Experimental Methods

2.1.1 Microdialysis system setup

Syringe pumps (CMA 4004, CMA Microdialysis AB, Solna, Sweden) were used, in combination with syringes (10 and 5 ml, Hamilton, Bonaduz, Switzerland) and microdialysis probes (CMA 20 Elite) with a polyarylethersulphone membrane (10 mm long, 500 μm outer and 400 μm inner diameter). For the collection, 500 μL plastic vials were used as dialysate. In every dialysate, MUF concentration was measured by fluorimetry (465nm emission at 360nm excitation) using a Spark fluorimeter (Tecan, Männedorf, Switzerland). Before using the microdialysis probes they were placed in a beaker with ultrapure water and perfusate with ultrapure water for 20 min to activate them.

2.1.2 The MUF-equilibration experiment

In the MUF–substrate solution, a certain amount of free MUF is always present. When collecting the perfusate, the measured MUF concentration includes both the MUF originally in the solution and the MUF released by enzymatic cleavage. Because the presence of free MUF also affects the flux dynamics of MUF in the microdialysis system over time, it is not sufficient to simply subtract the initial MUF concentration in the perfusate from the concentration measured in the dialysate. To investigate the relationship between MUF concentrations in the perfusate, in the external solution, and in the collected dialysate, we designed a MUF equilibration experiment testing multiple combinations of these parameters. The setup consisted of a microdialysis probe immersed in Eppendorf vial containing 500 μL of solution, with five different MUF concentrations ranging from 2.9 μM to 26.14 μM. In this setup, depletion or accumulation of MUF around the probe is allowed to occur over time. During a period of 90 min, we perfuse the tube at a flow rate of 2.5 μL/min using five different MUF concentrations ranging from 0 to 24 μM. The goal is to determine the equilibration behavior of MUF when it is present both inside and outside the microdialysis probe. A dialysate sample is collected every 45 minutes, and the MUF concentration is measured. In addition, the final concentration of MUF outside the membrane is measured after the experiment. By knowing the initial and final MUF concentrations outside the probe (in the surrounding aqueous solution), as well as the MUF concentrations in the perfusate (input) and in the dialysate (output), we can calculate the system's loss rate using the following equation:

$$\text{Loss rate } (\%) = \frac{C_{\text{retrieved}}}{C_{\text{introduced}}} \cdot 100, \tag{2}$$

where $C_{\text{introduced}}$ refers to the total amount of MUF (in μmol) introduced into the system via the perfusate and the initial Eppendorf vial solution, and $C_{\text{retrieved}}$ refers to the total amount of MUF (in μmol) found at the end of the experiment, including what remains in the Eppendorf vial and what is recovered in the dialysate.

2.1.3 Sampling

Soil cores were collected twice, on 1^{st} September 2024 and 5^{th} May 2025, from a beech forest near Vienna, Austria (48°16′ N, 16°19′ E). During the first sampling, the soil temperature was 16.4 °C with a water content of 11.88 %(±3.35). In contrast, in May, the soil temperature was 10.2 °C, and the water content was of 30 %(±2.3). On both days, the soil pH ranged from 6.121 to 6.827. Steel corers (10 cm i.d., 6 cm height) were used to extract soil cores from the upper 6 cm of topsoil within a 16 m^2 area. At four (May) and five (September) randomly selected locations within this area, triplicate cores were taken side by side. To preserve the natural structure and heterogeneity of the soil, we aimed to minimize disturbance during sampling. The corers containing intact soil samples were sealed on both ends with plastic lids and stored at 16 °C (September) and 23 °C (May) for a maximum of one week. Soil water content is a key parameter for microdialysis, as it ensures adequate contact between the microdialysis membrane and the soil. One day before the start of the experiment using the September core samples, 68 g of ultrapure water was added to the cores using a pipette and distributed as evenly as possible around them. This resulted in a final water content of 32.25%(±4.83).

2.1.4 Conventional potential chitinase enzyme activity

To validate extracellular enzyme activity (EEA) estimates obtained from microdialysis measurements and to parameterize the diffusion model, we additionally quantified EEA using conventional soil slurry assays. Fresh soil from both sampling events was sieved through a 2 mm mesh, and 1 g of sieved soil was suspended in 50 mL of 50 mM sodium acetate buffer (pH 6.0). The slurry was homogenized using an ultrasonic probe calibrated to deliver 350 kJ of energy per sample. Enzyme activity assays were conducted in black polystyrene 96-well microplates (Greiner Bio-One, Frickenhausen, Germany), with four replicate wells prepared per slurry and six substrate concentrations. Each well received 200 ul of soil slurry and 50 μL of 4-Methylumbelliferyl N-acetyl--D-glucosaminide (MUF–NAG) at final concentrations of 2, 1, 0.5, 0.25, 0.125, and 0.0625 mM. MUF-NAG is a syn-

thetic substrate which substitutes chitin-oligomers. To measure the cleavage by the enzymes, we monitor the increase of MUF in solution. Fluorescence was measured immediately after substrate addition and again after 90 min. The increase during this time lapse, normalized per gram of soil and per minute, represents the EEA rate.

2.1.5 Michaelis Menten Microdialysis Enzyme Activity Experiment

To verify whether microdialysis is suitable for measuring EEA in situ, we tested whether it can reproduce a Michaelis–Menten curve by introducing different substrate concentrations to generate a saturation curve. This also provides information on the MUF–NAG range in which the reaction rate depends solely on enzyme concentration ([E]) rather than substrate availability. As in the conventional method, five different MUF-NAG concentrations in aqueous solution (8 mM, 4 mM, 2 mM, 1 mM, and 0.5 mM) were used as perfusates to achieve a similar concentration of substrate in the soil. We assumed a MUF-NAG transfer rate into the soil of 10% and a surrounding environmental volume of 500, μL. Under these conditions, the amount reaching the soil after 90 min results in a concentration of 400 μM of MUF-NAG in the outside tube, corresponding to the final concentration in the conventional method. In each of the four replicate soil cores of the september core samples, five microdialysis probes were inserted using a 0.5 mm needle, with a spacing of 1.5 cm between them. Each core was perfused for 180 minutes at a flow rate of 2.5 μL min^{-1}. Dialysate samples were collected every 45 minutes, and MUF concentrations were subsequently measured.

2.1.6 The Retrieval Experiment

The aim of this experiment was to quantify the fraction of MUF that can be recovered from the soil solution , versus the proportion lost to the soil through abiotic and biotic processes. In the first step, MUF was introduced into each soil core via microdialysis during a defined amount of time. The perfusate was then switched to water, and we measured how much of the introduced MUF could be retrieved back by inversing the concentration gradient. For this purpose, three microdialysis probes were inserted into each soil core sampled in May, positioned 4 cm apart and 2 cm from the core edge. It was assumed that the location of the probes in the soil was sufficiently separate during the experiment to consider all three probes independent. Before placing the microdialysis probe in holes made using 0.2mm syringe, the tip was dipped into ultrapure water. All probes were perfused at a flow rate of 2.5 μL/min. Before beginning perfusion with substances, the cores were perfused with ultrapure water for 20 min to allow the formation of a water bridge. This setup included two phases: the *introduction phase*, during which MUF at a concentration of 10, μM was

perfused into the soil, and the *retrieval phase*, during which ultrapure water was perfused and MUF was collected from the soil.

In each of the four replicate cores, two conditions were applied:

- In the first perfusate, MUF at a concentration of 10 μM was perfused for 45 min, followed by ultrapure water for 5×45 min.
- In the second perfusate, MUF at the same concentration was perfused for 6×45 min, followed by ultrapure water for 7×45 min.

In the introduction phase, the transfer rate was calculated as described by König et al. (2022):

$$\text{Transfer rate } (\%) = \frac{C_{\text{perfusate}} - C_{\text{dialysate}}}{C_{\text{perfusate}}} \cdot 100, \tag{3}$$

where $C_{\text{perfusate}}$ is the MUF concentration in the perfusate, and $C_{\text{dialysate}}$ is the MUF concentration in the dialysate. The transfer rate provides insight into the direction and magnitude of the flow between the inside and outside of the microdialysis probe. A negative transfer rate indicates flow from the outside into the probe, whereas a positive value indicates flow from the inside to the outside. The further the transfer rate is from zero, the stronger the net flow and the corresponding concentration gradient.

To estimate how much MUF can be retrieved after being introduced into the soil, the retrieval rate was calculated at the end of the experiment as (Wiesenbauer et al., 2024a):

$$\text{Retrieval rate } (\%) = \frac{C_{\text{retrieved}}}{C_{\text{released}}} \cdot 100, \tag{4}$$

where C_{released} refers to the total amount of MUF (in μmol) introduced into the soil via microdialysis during the introduction phase, and $C_{\text{retrieved}}$ is the MUF (in μmol) measured during the water-only collection phase in the collection phase. The retrieval gives information of the diffusion and the removal of MUF from the spot by abiotic processes.

2.1.7 Microdialysis Enzyme Activity Experiment

In this experiment, we aimed to measure chitinase activity in situ and investigate the effect of acetate and N-acetylglucosamine (NAG) additions on this exoenzyme activity using a "reverse" microdialysis approach (König et al., 2022). In each of the five soil cores of the May sampling, we placed three microdialysis probes, spaced 4 cm apart from each other and 2 cm from the core edge.

To prevent the soil cores from drying out, the upper surface was sealed with Parafilm. Small holes were perforated in the Parafilm using a 0.5 mm needle to allow for gas exchange. In each core, the three inserted probes received different treatments using different perfusate solutions:

- First perfusate: ultrapure water (control)
- Second perfusate: acetate (+Acetate)
- Third perfusate: NAG (+NAG)

Both NAG and acetate were applied at a C concentration of 500 mM C L^{-1}. Perfusion with the solutions was carried out for 4.5 hours and repeated every two days during the six-day experiment. On the final day, MUF-NAG was added to the perfusate at a concentration of 4000 μM to measure extracellular enzyme activity (EEA). This concentration was assumed to lie within the plateau phase of Michaelis–Menten kinetics, where the reaction rate depends only on enzyme concentration (Dick, 2011).

Thus, instead of the background solution, the following solutions were perfused:

- In the first perfusate, only MUF-NAG at a concentration of 4000 μM (control)
- In the second perfusate, MUF-NAG at a concentration of 4000 μM and acetate (+Acetate)
- In the third perfusate, MUF-NAG at a concentration of 4000 μM and NAG (+NAG)

Every 45 minutes of the 4.5 hours of the perfusion, one dialysate sample was collected and the MUF concentration measured.

2.2 `Individual-based` modelling of diffusion dynamics during microdialysis-based enzyme measurement in soil

We developed an individual-based mathematical model using `NetLogo` (v6.4.0) (Wilensky, 1999) to simulate reverse-microdialysis measurements of extracellular enzyme activity (EEA). The aim was to better understand solute dynamics in and around the microdialysis probe and to aid interpretation of experimental results. The model simulates the transport and transformation of two chemical species, MUF–NAG (substrate) and MUF (product), in environments with different properties. In general, the goal is to replicate experiments in which the probe is immersed in different surrounding media, such as an aqueous solution, a soil slurry, or intact soil cores. These different media vary in the space available for diffusion.

The model incorporates both molecular transport and reaction processes. Transport includes (i) advection of solutes within the microdialysis probe, (ii) diffusion across the probe membrane, and (iii) diffusion through the surrounding soil or solution. Reactions include enzymatic cleavage of MUF–NAG to MUF, as well as adsorption of MUF to the probe membrane.

2.2.1 Model domain and setup

The model is composed of a 2D grid, which represents the cross section of a soil core with dimensions $L_g \times h_g = 16.5 \times 23.5$ mm (see Fig. 3). Each cell is assigned one of four types: probe, pore, soil, or atmosphere. The tube, representing a CMA 20 Elite microdialysis probe (0.5 mm diameter, 1 cm length), is positioned at the center of the upper boundary of the grid and modeled as h_t cells wide and L_t cells long.

At the interface between the probe and the surrounding soil, solutes can diffuse across the boundary according to their respective concentration gradients, allowing exchange between the probe and the external medium.

To represent a diffusion volume, the 2D grid was defined with cells of diameter $\Delta x = 0.46$ mm and extended with an artificial depth of $\Delta d = 0.46$ mm. This created a pseudo-3D domain that enabled volume-dependent diffusion. In this model, the continuous system is approximated by discrete cells, which introduces a discretization error that increases proportionally with Δx. The cell size was therefore chosen as a compromise: small enough to minimize error, but large enough to keep simulation times computationally feasible. To ensure that discretization did not bias the results, we tested two different cell sizes and found consistent outcomes (see Supplement 4).

Simulations proceed in discrete time steps, with transport and reaction processes updated iter-

atively at each step. Each grid cell tracks concentrations of MUF, MUF–NAG, and enzymes. Enzyme concentration is constant, spatially fixed, and user-defined at initialization. MUF and MUF–NAG diffuse between cells according to their respective diffusion coefficients.

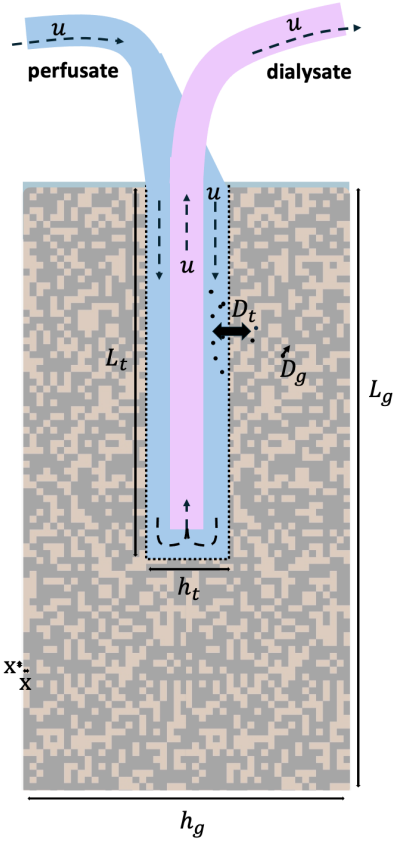

Name	Description	Value	Units
L_g	length of model grid	46.5	mm
h_g	diameter of model grid	23.5	mm
L_t	length of the micodialysis probe	10	mm
h_t	diameter of microdialysis probe	0.46	mm
u	volumetric flow rate	2.5	μL/min
Δt	second per time step	10	s
Δx	grid cell diameter	0.46	mm
Δd	grid cell depth	0.46	mm
D_t	Diffusion coefficient between probe and solution	-	mm^2/s
D_g	Diffusion coefficient within solution	-	mm^2/s
d_{max}	distance from the probe to the system's boundary	-	mm
P	Porosity, ratio of the number of pores to the number of cells	-	%

Figure 3: Schematic overview and table of model parameters. "–" indicates that the parameter is user-defined or has multiple options, as for the diffusion coefficient (two different molecules).

2.2.2 Senarios used: Solution and Core

The model was designed to represent two experimental scenarios: (i) a microdialysis probe tip (0.5 cm diameter, 1 cm length) inserted into an aqueous solution, and (ii) the same probe inserted into an intact soil core. These scenarios differ in both diffusion distance and accumulation dynamics, because the grid has closed boundaries. Incorporating different diffusion volumes is therefore essential to account for differences in MUF recovery.

In the aqueous solution scenario, the system represents a water volume of 500 μL surrounding the probe, consistent with the experimental setup. In contrast, the diffusion volume in soil cores is unknown and depends strongly on soil type, structure, and water content. Molecules cannot diffuse as far, since water pathways are only partially connected and pore structure constrains diffusion

(Nunan, 2017; Nunan et al., 2020; Moldrup et al., 2003).

To capture these differences, we introduced two adjustable parameters: (i) distance from the probe to the system's boundary $d_{\max}$, would define system's volume, i.e. the maximum distance (in Δx) from the probe within which molecules can diffuse, and (ii) porosity, defined as the fraction of grid cells designated as pores during initialization (for a schematic overview, see Fig. 4). Molecules are restricted to pore cells, as diffusion only happens in water-filled pores. Note that $d_{\max}$ ranges from 1 to 80 grid cells, whereas in the horizontal direction the maximum grid distance is 24, and in the vertical direction it is 80 grid cells. Thus, when we set $d_{\max}$ to 70, the maximum in the horizontal direction remains 24, as shown in Fig. 4.

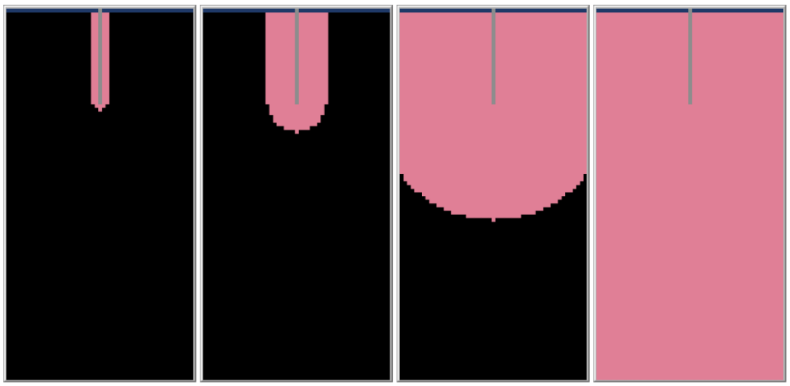

(a) For different values of the outer container radius ($d_{\max}$): 2, 8, 32, and 80 grid cells. The system's volume is shown in pink, and the grey grid cells represent the probe tip.

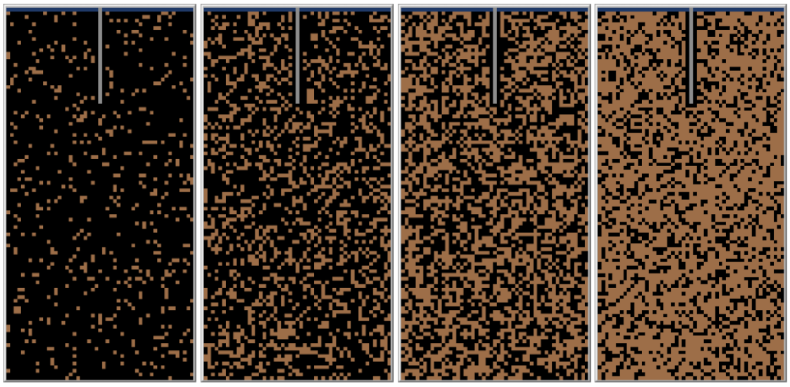

(b) For different porosity levels: 90%, 70%, 50%, 30%. The soil pores are shown in black, the solid soil particles in brown, and the grey grid cells represent the probe tip.

Figure 4: Overview of the grid setup depending on the parameter d_{max} and porosity.

In practice, we defined the model "core" environment as having a smaller diffusion radius (d_{max} = 0.5 cm) combined with a porous space in which 45% of the cells were designated as pores (see Fig. 5). This simplified representation is not intended to match experimental soil cores precisely, but

rather to approximate their reduced system's volume ($d_{\max}$) and structural constraints relative to the aqueous solution in model simulation.

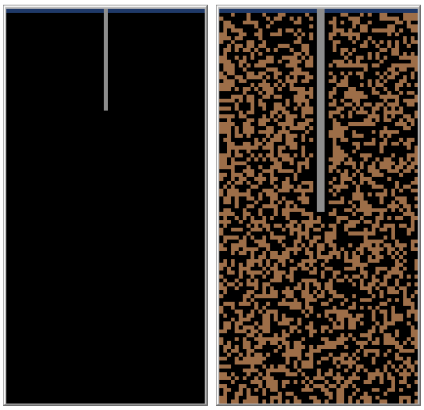

(a) **Solution** (b) **Core**

Symbol	**Solution**	**Core**	Units
d_{max}	3	0.5*	cm
porosity	100	45*	%
V_g	497.35	39.4*	μL

(c) Values used in model; * indicates that these values are not experimentally derived.

Figure 5: Grid layout depending on the experimental set-up and grid variables

2.2.3 Transport

In our model, we consider three coefficients that describe distinct types of molecular movement (see Figure 3): transport via perfusion of the solution inside the probe (u), diffusion of molecules within the soil matrix (D_g), and diffusion between the probe and the soil (D_t). First, the calculations are presented in a general form, independent of grid size.

Volumetric flow rate To represent perfusion inside the probe, we modeled the transport of solution as discrete drops of liquid, each with the volume of a grid cell, that move through the system. According to the specified flow rate (u), a certain volume of perfusate is pumped into and out of the tube. Typically, the volumetric flow rate used ranges between $1 - 20\ \mu L/min$ and for the simulation we applied $2.5\ \mu L/min$. Consequently, a drop of liquid with a volume of Δx^3 which moves through a number of grid squares per time step, which is calculated as follows:

$$u_{\text{grid}} = \frac{u}{\Delta x^3} \cdot \frac{\Delta t}{60} \qquad \left[\frac{\Delta x^3}{\Delta t}\right] \tag{5}$$

Diffusion in the grid The second two diffusion coefficients are driven by concentration gradients and can be described using Fick's law (6):

$$J = -D\frac{\Delta c}{\Delta r} \tag{6}$$

where D is the diffusion coefficient, Δc the concentration difference, and Δr the distance over which diffusion occurs (Bungay et al., 1990). The diffusion from the probe into the soil is not identical to diffusion within the soil solution, as it is regulated by the presence of a semipermeable membrane and the flow rate of the liquid in the tube.

To estimate the diffusion rates of MUF and MUF–NAG outside the probe as a function of molecular size, we approximated both molecules as spherical particles and applied the Stokes–Einstein equation. The relationship between the diffusion rate D and the size of the molecule (spherical particle) (Evans et al., 2018) is given by the Stokes–Einstein equation (7):

$$D = \frac{k_B T}{6\pi\eta r_H} \tag{7}$$

where k_B is the Boltzmann constant, T is the temperature of the solvent in Kelvin, η is the dynamic viscosity of the solvent, and r_H is the radius of the diffusing molecule.

Assuming room temperature is 22.5 $°C$ and the water viscosity at this temperature is equal to $0.9455 \times 10^{-3}\ \mathrm{kg\,m^{-1}\,s^{-1}}$. Lastly, the Stokes radius can be approximated by:

$$r_H = c \cdot M^{\frac{1}{3}} \tag{8}$$

where M is the molecular weight of the molecule and c an unknown constant to be determined. For this determination, we need to use a molecule for which the molecular weight and diffusion coefficient are known. We chose phosphate because it has a known diffusion coefficient of $D = 2.470 \times 10^{-9}, \mathrm{m}^2, \mathrm{s}^{-1}$ at a temperature of $298, \mathrm{K}$ (Kadhim and Gamaj, 2020), and a molecular weight of $94.97, \mathrm{g}, \mathrm{mol}^{-1}$. Thus, the constant c is equal to 0.5×10^{11}.

Having determined the parameter c, we can approximate the diffusion coefficients of MUF and MUF–NAG using their molecular weights in combination with the Stokes–Einstein equation. The resulting values for MUF–NAG and MUF are presented in Table 1.

In NetLogo, diffusion is implemented as the fraction of concentration that leaves a patch at each time step and is equally distributed among its eight neighboring patches. If a neighboring patch does not exist (e.g., at the border or in a non-pore cell), the share that would have diffused into it

remains in the original patch. Converting units of diffusion coefficient from m^2/s to $\Delta x^2/\Delta t$:

$$D_g = D \cdot 10^{-12} \left[\frac{m^2}{s}\right] = \frac{D}{\Delta x^2} \cdot 10^{-6} \cdot \Delta t \quad \left[\frac{\Delta x^2}{\Delta t}\right] \tag{9}$$

Substance units	M g/mol	$D \cdot 10^{-12}$ m^2/s	D_{g} $\Delta x^2/\Delta t$	D_{t} $\Delta x^2/\Delta t$
MUF-NAG	379.4	1613	0.08	0.02
MUF	160.17	2144	0.10	0.06

Table 1: Diffusion coefficients

Diffusion between probe and soil The flux between the probe and the soil depends on several probe- and solute-specific parameters, such as membrane properties and perfusion flow rate, and therefore must be determined empirically (Shippenberg and Thompson, 1997; Bungay et al., 1990). This is done using the recovery rate (RR), which quantifies the percentage of solute recovered in the dialysate relative to the external solution:

$$RR\ (\%) = \frac{C_{\mathrm{dialysate}}}{C_{\mathrm{outside}}} \cdot 100, \tag{10}$$

where $C_{\mathrm{dialysate}}$ is the solute concentration in the dialysate and C_{outside} that in the external medium. Alternatively, RR can be expressed as a function of the mass transfer coefficient K_0, the active membrane area A, and the flow rate u (Shippenberg and Thompson, 1997):

$$RR\ (\%) = \left(1 - e^{-\frac{K_0 \cdot A}{u}}\right) \cdot 100, \tag{11}$$

with $A = A_{\mathrm{total}} \cdot \rho$, where ρ is the fraction of the membrane that is active. From this relationship, we define the effective probe–soil diffusion coefficient D_t as:

$$D_t = \frac{K_0 \cdot \rho \cdot A_{\mathrm{total}}}{u}. \tag{12}$$

To parameterize D_t, we used recovery rate experiments performed previously by Thayer Taft following (Wiesenbauer et al., 2024a; König et al., 2022). Recovery rates were measured at different flow rates, and the data were fitted to estimate $K_0 \cdot \rho$ (Figure 6). These fitted values were then used to calculate D_t for a flow rate of 2.5 μL/min (Table 1).

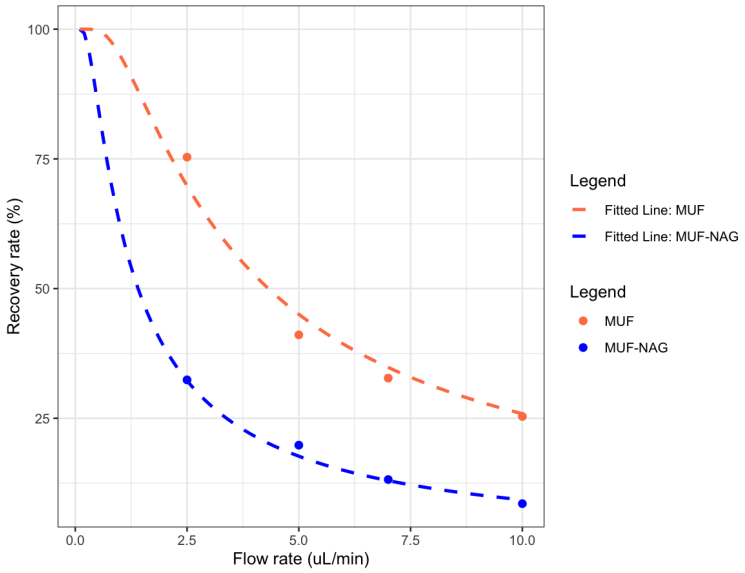

Figure 6: Recovery rate fitting for MUF-NAG and MUF. Dots represent experimental results; the dashed curve represents the fitted model.

2.2.4 Reaction

Enzyme kinetics Outside the probe, whether in soil or in solution, enzymes are assumed to be present and to cleave MUF–NAG. In the model, enzymes are assumed to be homogeneously distributed across the grid and unable to diffuse, which simplifies the strong spatial heterogeneity expected in real soils. At every time step, substrate is converted to MUF according to Michaelis–Menten kinetics:

$$v = \frac{[E] \cdot [\text{MUF-NAG}] \cdot v_{\max}}{[\text{MUF-NAG}] + K_m}, \tag{13}$$

where v is the reaction rate, $[E]$ the enzyme concentration, [MUF-NAG] the substrate concentration, $v_{\max}$ the maximum turnover rate, and K_m the michaelis constant. For the model we use the parameters derived from the conventional essay provided by previous experiments. Having 4 replicates S1, S2, S3, S4 from the same 16m^2 spot in the forest, yielding the activity curves shown in Figure 7. From these data, the Michaelis constant K_m, the substrate concentration at which the reaction rate is half of $v_{\max}$, was reached at around the addition of 50 μL of 0.25 mM MUF-NAG to a 200 uL soil slurry, corresponding to a final solution concentration of 0.05 mM. Based on this, we set $K_m = 0.05$ mM for the model. The other key parameters, $v_{\max}$ and the enzyme concentration $[E]$, jointly determine the maximum height of the reaction plateau. In the model, they are combined into a single effective parameter, $v_{\max} \cdot [E]$, which can be adjusted by the user.

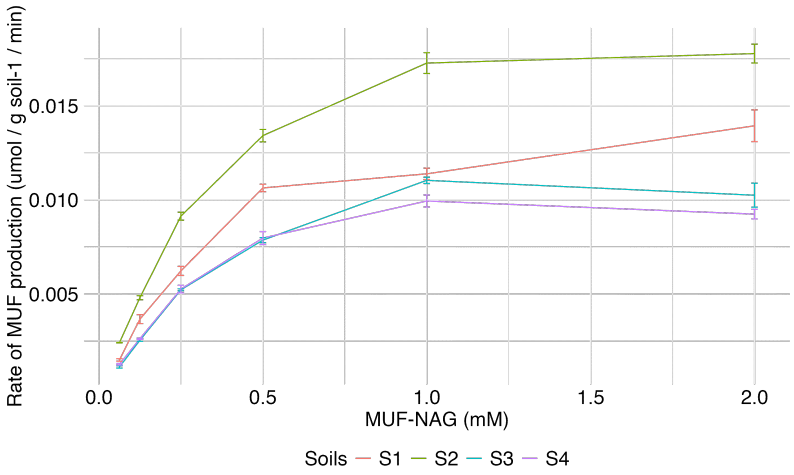

Figure 7: **conventianally measured chitinase kinetics** Rate of MUF production in soil slurries over 90-min period after the addition of different concentration of MUF-NAG. S1, S2, S3, S4 are the 4 replicates from the same 16m^2 spot in the forest.

Sticking of MUF in the Tube One possible explanation for why the results of the MUF equilibration experiment (see Section 3.2.1) did not align with our expectations or with the model outcomes is that MUF may have adhered to the walls of the microdialysis tubing. In other words, a portion of the MUF molecules may stick to the input and output tubes of the microdialysis system. We assume that this portion decreases over time as the sticking area in the tube becomes increasingly saturated.

The sticking behavior follows this equation,

$$s(t) = s_0 \cdot e^{-t \cdot s_m} \tag{14}$$

where s_0 is the initial or maximal sticking rate, and s_m is the decay constant. After fitting the model to the data points of the MUF-equilibration experiment by minimizing the mean squared error of the intersection, s_0 was set to 0.5 and s_m to 0.0015.

Results

3.1 The Microdialysis System: A Model Analysis

The MUF collected in the dialysate (output) results from multiple processes, including diffusion through different media and enzymatic reactions. The biggest challenge is to disentangle these processes in order to isolate the fraction of MUF originating from enzymatic activity. Unfortunately, all factors interplay and depend on parameters that cannot be directly measured experimentally. However, the model allowed us to investigate some factors in detail, including: (i) the system's volume influenced by the probe size, (ii) the MUF–NAG (substrate) concentration within the core, (iii) the contribution of MUF (product) already present in the perfusate (input) to the dialysate (output), and (iv) the effective extracellular enzyme activity (EEA) around the membrane. Each of these factors can influence the MUF recovered in the dialysate and must be understood to establish microdialysis as a reliable method for measuring enzyme activity.

Since many of these factors are impossible to measure directly in intact soil cores, the model provides a framework to systematically vary them and explore their influence on the outcome. In this part we use the model for the following analysis:

- How does the recovery of MUF depends on the volume available outside for diffusion?
- How does MUF already present in the perfusate influence the MUF in the output?
- What is the impact of enzyme activity on the transfer rate?

System's volume One factor that affects the amount of MUF collected in the dialysate is the system's volume, which corresponds to the amount of water around the probe. The effect of volume on MUF recovery is not straightforward. On one hand there is more place for MUF to diffuse, this can slow down the recovery. On the other hand there are more enzymes to be reached. In the model, this volume can be modified in two ways: (i) the radius of the container around the probe, in which molecules can diffuse (ii) the porosity, which alters the soil structure by reducing the pore space available around the probe (see Fig. 4 and for more details of the implementation see Section 2.2.2).

We consider that MUF enters the system through the perfusate and diffuses into the surrounding solution. To explore this, we first consider a simplified scenario without enzymatic activity. Over time, MUF accumulates around the membrane until the surrounding solution is saturated and no more MUF diffuses out of the probe. At this point, the MUF concentration outside the probe

equals the MUF concentration inside, and diffusion is balanced. For example, with 10 μM MUF in the perfusate and no extracellular enzyme activity, equilibration is reached once the MUF concentration in the dialysate has risen to 10 μM. The time of this equilibration depends on the system's volume. To look at the effect of this, we simulated this set-up with different radius for the solution container ($d_{\max}$), this in turn changes the total volume, and therefore the diffusive dynamics. The time required to reach equilibrium depends on the system's volume. As shown in Fig. 8, equilibration time increases nonlinearly with volume. Our experiments however, are time constrained, lasting at most 270 min (4.5h), we focus on the volumes for which equilibration is reached within this timeframe. Only for volume below 30 μL equilibration was achieved in less than 270 min (Fig. 8b). A volume of 30 μL corresponds to a location approximately 2.3 mm away from the probe within the 2D grid cell, from which the molecule can diffuse.

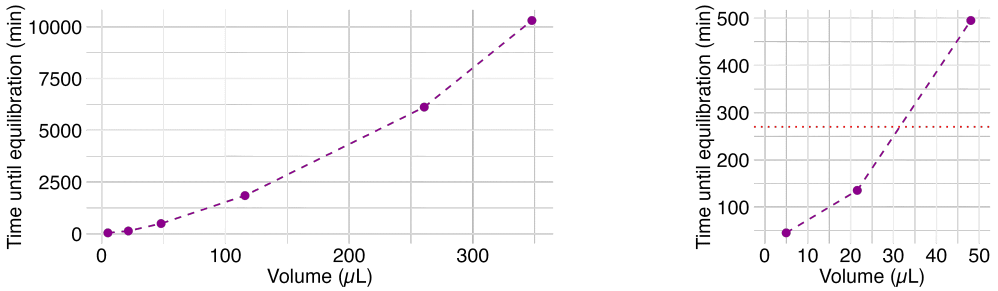

(a) (b)

Figure 8: **Simulation** – (a) Time to reach equilibration (min) as a function of the outside effective volume, varied by changing the radius of the outside container. (b) Zoom-in of (a) for volumes below 50 μL. The dotted red line indicates the equilibration time used in our experiments (270 min). As shown, it intersects the dashed curve at about 30 μL, defining the maximum volume at which the concentrations inside the solution and in the probe reach equilibrium.

One step further, we now examine a similar setup in solution, but this time including enzymatic reactions. Additionally to the MUF, MUF-NAG enters the system through the perfusate, diffuses into the solution, and is cleaved by enzyme, this releases MUF. In this setup, MUF outside the probe therefore has two sources: diffusion from the perfusate and enzymatic cleavage. Because enzymes increase MUF accumulation around the probe, we tested whether system's volume influences how much MUF is ultimately collected when the enzyme concentration outside is kept constant across all simulations. To this end, we analyzed the MUF collected (μM) over 270 min, which is also the experimental duration of interest.

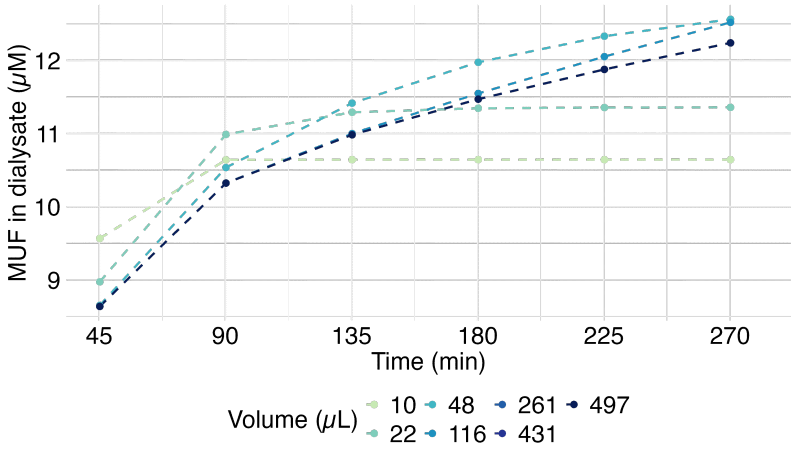

Figure 9: **Simulation** – MUF collected (μM) in the dialysate over 270 min (4.5 h) of perfusion with $[E] \cdot v_{\max} = 0.025$, for different outside effective volumes obtained by varying the radius of the outside container.

For system's volumes below 50 μL, MUF in the dialysate stabilizes over time, as the surrounding volume becomes saturated with MUF and all available enzymes are occupied (Fig. 9). Within this range, the plateau reached for the larger container volume (22 μL) is higher than for the smaller volume (10 μL). This is because in a larger volume more enzymes are available, and therefore more MUF is cleaved. In contrast, for volumes of 261 μL or larger, the curves completely overlap, showing that the system boundaries have not yet influenced the dynamics and would only become relevant over longer timescales.

Overall, the pattern is consistent: smaller volumes reach equilibrium faster. Once saturation at the boundaries begins, the recovered MUF rises more quickly before reaching a plateau. In contrast, for larger volumes, where the system boundaries are farther away, no significant accumulation occurs within this time frame, and MUF increases more steadily. For example, after 135 min, the MUF in the dialysate for a volume of 261 μL begins to rise more sharply, indicating the onset of boundary effects. Indeed, looking at the MUF distribution around the probe after 270 min in Fig. 11, the boundary effect due to $d_{\max}$ is more clearly visible at 116 μL than at 497 μL, indicating that accumulation at the boundary has begun.

All these dynamics are reflected in the MUF collected (μM) after 270 min: showing a sharp increase at low volumes, followed by a decrease due to boundary saturation (shortly increasing the MUF recovered), and finally a plateau (Fig. 10). In conclusion, smaller volumes lead to faster accumulation and thus reach equilibrium sooner, but the final equilibrium level is lower.

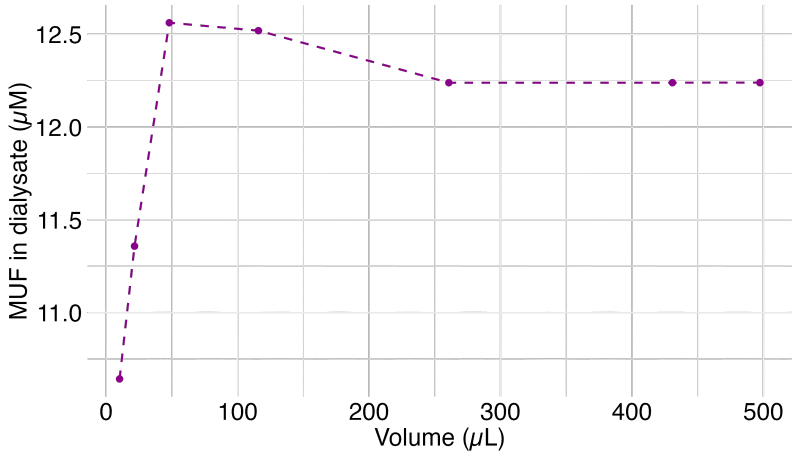

Figure 10: **Simulation** – MUF collected (μM) in the dialysate over 270 min (4.5 h) of perfusion with $[E] \cdot v_{\max} = 0.025$, for different outside effective volumes obtained by varying the radius of the outside container.

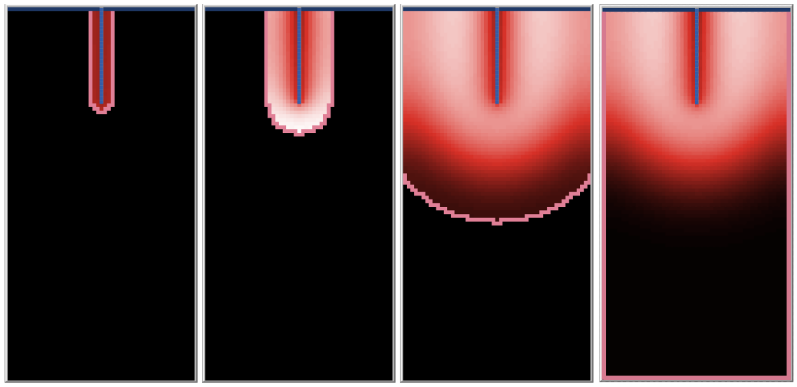

Figure 11: **Simulation** – Overview of the distribution of outside MUF (μM) after 4.5 h of perfusion with $[E] \cdot v_{\max} = 0.025$, shown for different outside effective volumes (10, 48, 116, and 497 μL), obtained by varying the radius of the outside container. The pink grid cells indicate the boundaries of the effective volume used in the simulation. MUF concentration is shown in red, with lighter colors corresponding to higher concentrations.

Another way to alter the system's volume is by changing the porosity of the surrounding environment (see Fig. 4). As porosity decreases, fewer pores are present in the grid, reducing the system's volume around the probe and distorting diffusion pathways because molecules can move only within pores. Note that the porosity, also creates disconnection between pores, leaving some pores inaccessible to substances diffusing out of the probe (see Fig. 4). Thus, the effective system's volume is calculated as the volume of the pore cells that are reachable from the probe. In this scenario, we kept the same maximum d_{max} (so that the potential diffusion space equals 500 μL).

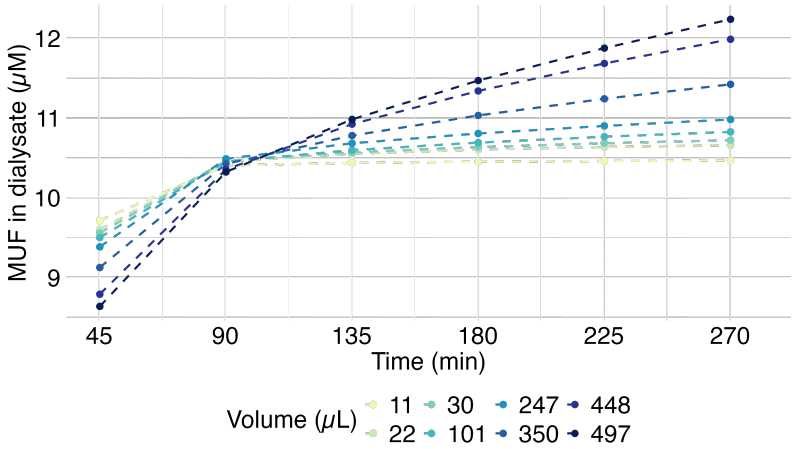

Figure 12: **Simulation** - MUF collected (μM) in the dialysate over 270 min (4.5 h) of perfusion with $[E] \cdot v_{\max} = 0.025$, for different outside effective volumes obtained by varying the porosity of the outside. The effective system's volume is calculated as the volume of the pore cells that are reachable from the probe.

The temporal dynamics differ from those observed when changing $d_{\max}$ (see Fig. 9). This is mainly because changing the radius alters the boundaries, without affecting diffusion immediately around the probe. In contrast, changing the porosity directly influences diffusion and accumulation patterns in the proximity of the probe. Considering the effect of porosity: at the beginning, lower system's volumes (i.e., lower porosity) collect more MUF because accumulation around the probe is stronger, which increases recovery (Fig. 12). After approximately 112 minutes, however, larger volumes collect more MUF and show a faster increase in recovery over time. This is because the effect of reaching more enzymes is now becoming apparent. This effect is visually clear in Fig. 14: after 4.5 hours of perfusion, higher porosity allows MUF to diffuse farther, producing a less distorted concentration gradient. As a result, the MUF collected after 4.5 hours increases with volume (see Fig. 13), ranging from 10.3 to 12.23 μM.

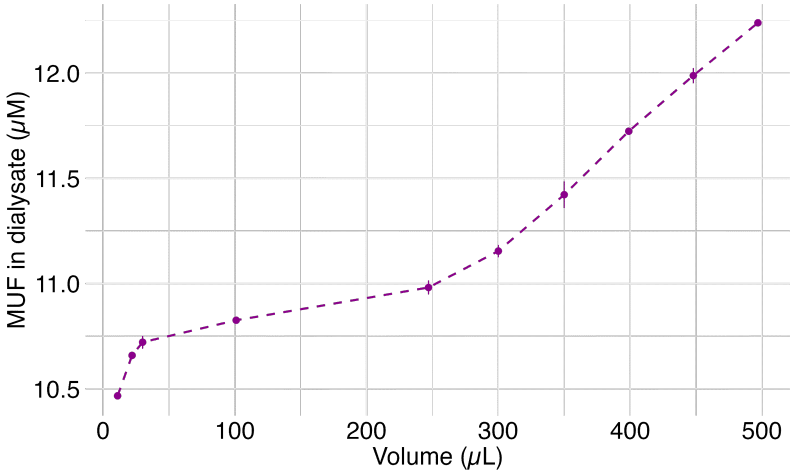

Figure 13: **Simulation** – MUF collected (μM) in the dialysate after 270 min (4.5 h) of perfusion with $[E] \cdot v_{\max} = 0.025$, for different outside effective volumes obtained by varying the porosity of the outside. The effective system's volume is calculated as the volume of the pore cells that are reachable from the probe. Error bars represent the standard deviation from 5 simulation runs for each condition.

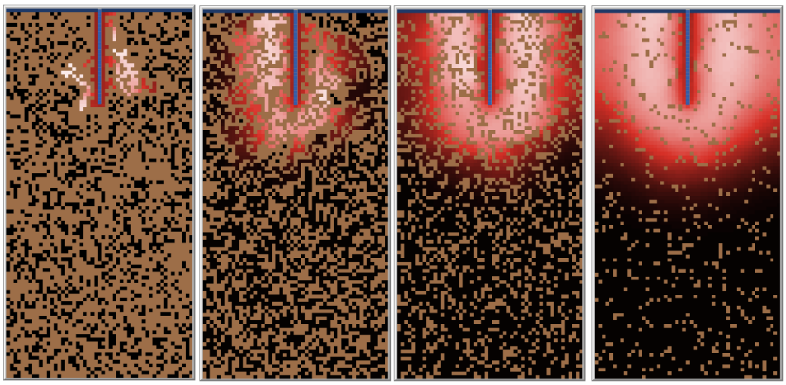

Figure 14: **Simulation** – Overview of the distribution of outside MUF (μM) after 4.5 h of perfusion with $[E] \cdot v_{\max} = 0.025$, shown for different outside effective volumes (11, 247, 350, and 497 μL), obtained by varying the porosity of the outside container. The effective system's volume is calculated as the volume of the pore cells that are reachable from the probe. MUF concentration is shown in red, with lighter colors corresponding to higher concentrations.

Contribution of MUF in the perfusate. One of the main challenges in using reverse microdialysis to measure EEA is accounting for MUF already present in the perfusate. The model allows us to simulate two scenarios: a "clean" perfusate containing no MUF, and a "non-clean" perfusate containing 10 μM MUF. In both cases, $[E] \cdot V_{\max}$ and the outside volume are kept constant, using the solution volume without porosity and an effective system's volume of 500 μL, equivalent to the amount of water in the Eppendorf vial used in the experiment. This allows us to understand how the presence of MUF alters the flux dynamics in the system.

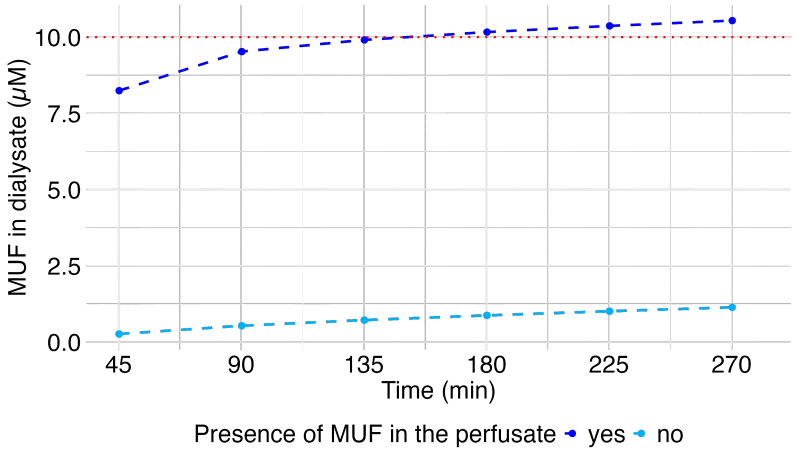

Figure 15: **Simulation** - The influence of the MUF presence in the perfusate on the MUF collected in the dialysate. Parameters: 4000 μM MUF-NAG concentrations with an additional 10μ M MUF concentration (marked as a red dashed line) in the same solution volume with $[E] \cdot V_{\max} = 0.01$.

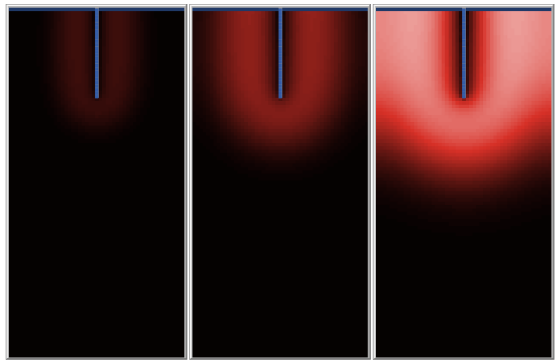

(a) No MUF present in the perfusate

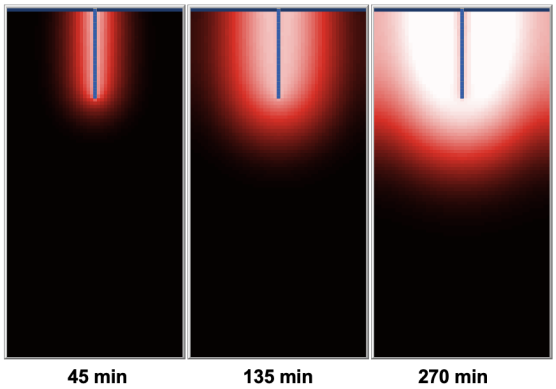

(b) MUF present in the perfusate

Figure 16: **Simulation** – Overview of the distribution of outside MUF (μM) over time in the model grid. MUF concentration is shown in red, with lighter colors indicating higher concentrations. Parameters: 4000 μM MUF-NAG, with an additional 10 μM MUF in the same solution volume, and $[E] \cdot V_{\max} = 0.01$.

In the case when there is no MUF in the perfusate, all MUF collected results only from enzymatic cleaving, while in the second case it originates from both enzymatic cleaving and the perfusate. In

the second case, which is the case of our experiment, we have to understand its sources and the temporal dynamics. In the second case, at the beginning, the amount collected is lower than the perfusate concentration, as MUF initially diffuses from the probe into the surrounding medium (Fig. 16). After a critical time point of 152 min, this direction reverses, indicating that the MUF concentration outside is higher than in the perfusate. This surplus can only originate from enzymatic cleavage outside the probe. As shown in Figure 15, MUF in the dialysate increases with time in both scenarios. However, when MUF is present in the perfusate, the total amount recovered is always higher and the time course shows a steeper increase. The results of the model show that a simple subtraction of perfusate MUF from dialysate MUF cannot provide a valid correction, because the relative contributions of perfusate, diffusion and enzymatic cleavage change dynamically over time.To investigate the relationships between MUF in the perfusate, the surrounding solution, and the dialysate, we conducted both an experiment and a model simulation. We combined various MUF concentrations in the perfusate and the surrounding solution and analysed their combined effect on MUF in the dialysate (see Section 3.2).

Influence of extracellular Enzyme Activity Our main factor of interest is the active extracellular enzyme concentration outside the probe. This parameter is unknown in soil cores, but estimating it, or at least comparing relative EEA levels within the same soil, where the system's volume is approximately constant, is the primary objective of microdialysis measurements. This allows us to understand how the presence of MUF alters the flux dynamics in the system. To track this, we used the transfer rate as a proxy. The transfer rate reflects both the direction and magnitude of flux: a positive value indicates net movement from the probe into the soil, while a negative value indicates net flux from the soil into the probe. The further the transfer rate is from zero, the stronger the concentration gradient between the probe and the surrounding soil.

In the model, we simulated different EEA levels by assigning various values to $[E] \cdot v_{\max}$ and introducing a MUF–NAG concentration of 4000 μM simultaneously with 10 μM of MUF. The outside volume was kept constant, using the solution volume without porosity and an effective system's volume of 500 μL.

The temporal dynamics of transfer rates followed a consistent pattern: rates gradually declined over time (Fig. 17). At the beginning of the simulation, no MUF was present outside the probe because MUF–NAG had not yet been cleaved. Consequently, the perfusate concentration exceeded that of the surrounding soil, and net flux was directed outward. As enzymatic cleavage progressed, MUF accumulated outside the probe, reversing the gradient and shifting flux inward, which produced

increasingly negative transfer rate values. This reversal occurred more rapidly and with greater magnitude under higher EEA, reflecting the steeper concentration gradient generated by faster MUF production.

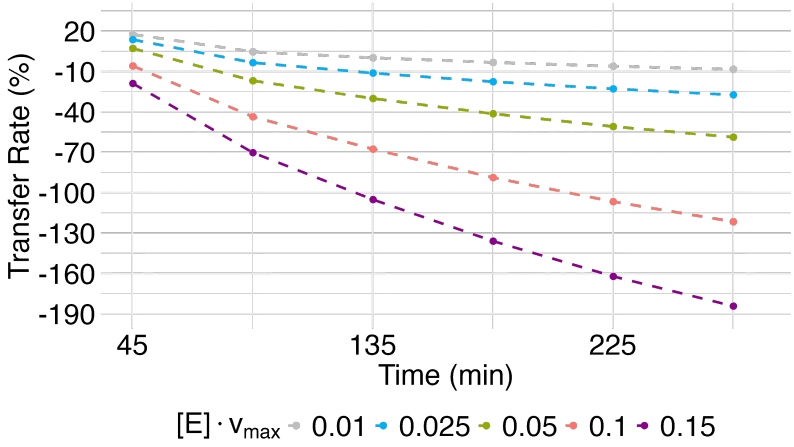

Figure 17: **Simulation** - Temporal dynamics of the transfer rate of MUF over six dialysates with five different $v_{\max} \cdot [E]$ values.

Summary The model analysis shows that unknown factors such as volume, porosity, and enzyme abundance in the surrounding environment strongly influence the recovered MUF. We also demonstrated that MUF transfer from the perfusate to the dialysate is dynamic and does not follow a simple proportional relationship.

3.2 Solution Experiments and Calibration

3.2.1 The MUF-equilibration experiment: One case study

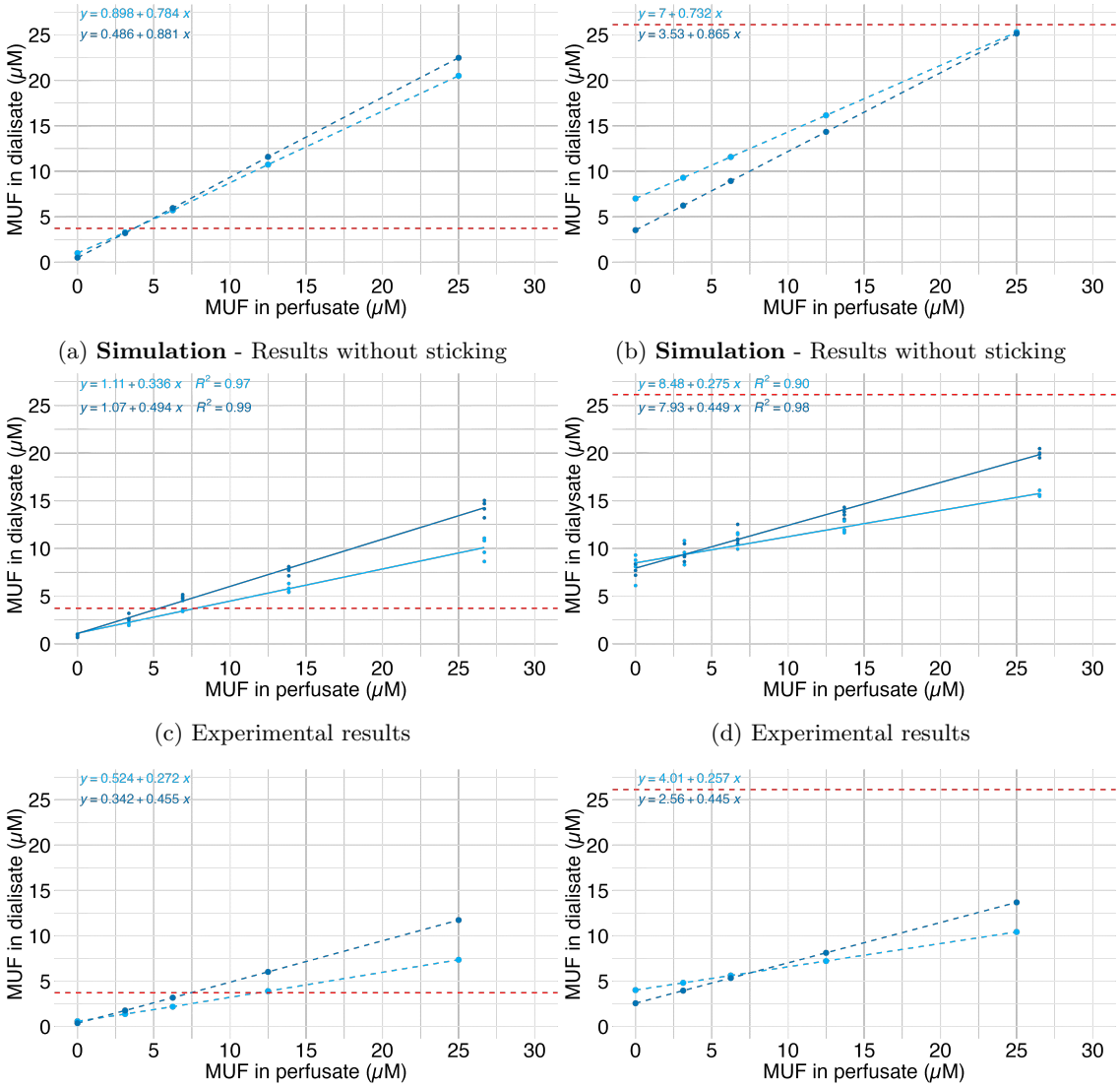

(a) **Simulation** - Results without sticking

(b) **Simulation** - Results without sticking

(c) Experimental results

(d) Experimental results

(e) **Simulation** – Results with sticking, using parameters $s_0 = 0.5$ and $s_m = 0.0015$.

(f) **Simulation** – Results with sticking, using parameters $s_0 = 0.5$ and $s_m = 0.0015$.

Figure 18: Relationship between MUF (μM) in the perfusate and in the dialysate at two time points (45 min and 90 min), shown for two initial outside MUF concentrations: (a), (c), and (e) 3.72 μM, and (b), (d), and (f) 26.13 μM, indicated by the red dashed line.

In this section, we present a preliminary reverse microdialysis experiment performed not in a soil core but in an Eppendorf vial containing 500 μL of solution. The objective was to determine how much MUF appears in the dialysate (output) for given MUF concentrations in both the external solution and the perfusate (input), thereby characterizing their temporal interplay. In the context of measuring extracellular enzyme activity in soil cores, the MUF in the perfusate is known, and

the MUF in the dialysate can be measured. The challenge is to distinguish MUF originating from enzyme activity from that already present in the perfusate. Resolving this relationship provides a basis for estimating the external MUF concentration that arises exclusively from enzymatic cleavage. Thus, we address the central question:

- Can we correct for MUF already present in the perfusate?

In Section 3.1, we have seen that the presence of a background concentration of free MUF in the MUF–NAG solution strongly affects the dynamic flux between the probe and its environment, causing the relative contributions of MUF from the perfusate to the MUF in the dialysate to change dynamically over time. Unlike in conventional assays, simple subtraction of the initial MUF concentration is not possible, as diffusion governs the system (see Fig. 15). At the start, no MUF is present outside the probe, while the perfusate contains MUF that diffuses outward. Consequently, MUF in the dialysate is initially lower than in the perfusate but increases over time due to both diffusion and enzymatic activity. This interplay requires careful calibration to separate MUF derived from the perfusate from that released by extracellular enzymes.

To test this, probes were inserted into 500 μL MUF solutions of known concentration and perfused with five different MUF concentrations. Dialysates were collected and analyzed after 45 and 90 minutes. For comparison, the same setup was also simulated using our model.

Looking first at the simulation results for external MUF concentrations of 3.72 μM and 26.13 μM, the model reproduced the expected dynamics (Fig. 18a & b). When the perfusate concentration was lower than the external concentration, flux was directed into the probe, leading to MUF depletion near the probe and reduced recovery in the dialysate over time. This is visible in Fig. 18a & b, where the light blue line (representing MUF collected after 45 min) is higher than the dark blue line (representing MUF collected after 90 min). When the perfusate concentration exceeded the external concentration, flux was reversed, resulting in the dark blue line being higher than the light blue line. At equal concentrations, no net flux was expected and a stable recovery over time, which corresponds to the MUF concentration in the perfusate. This pattern is visible in Fig. 18a & b, where the light blue line (recovery at 45 min) intersects the dark blue line (90 min) near $(3.72, 3.72)$ or $(26.13, 26.13)$, respectively.

In contrast, the experimental data (Fig. 18c & d) displayed a markedly different pattern: the intersection of both time points occurred at a much lower perfusate concentration of approximately 0.62 μM or 3.16 μM, respectively. Furthermore, while simulation slopes (Fig. 18a) ranged between 0.73 and 0.88, the experimental slopes were considerably lower, between 0.27 and 0.49.

Examining MUF distribution before and after the experiment further confirmed this discrepancy. In a closed system, any change in absolute MUF (μmol) between the perfusate and dialysate should be balanced by a corresponding increase or decrease in the surrounding solution. Yet, analysis of the loss rate (Fig. 19) revealed that 2.18–40.04% of MUF was unaccounted for, with losses increasing at higher perfusate concentrations. Together, these results indicate a potential adsorption of MUF to the microdialysis tubing.

To test this hypothesis, we incorporated sticking parameters $s_0 = 0.5$ and $s_m = 0.0015$ into the model (for details of the implementation, see Methods Section 3.2.1), implemented as a time-dependent loss of MUF within the tubing system. This modification decreased both the intersection point to 0.99 or 7.3 and the slopes of the perfusate–dialysate relationship (Fig. 18), consistent with the experimental data.

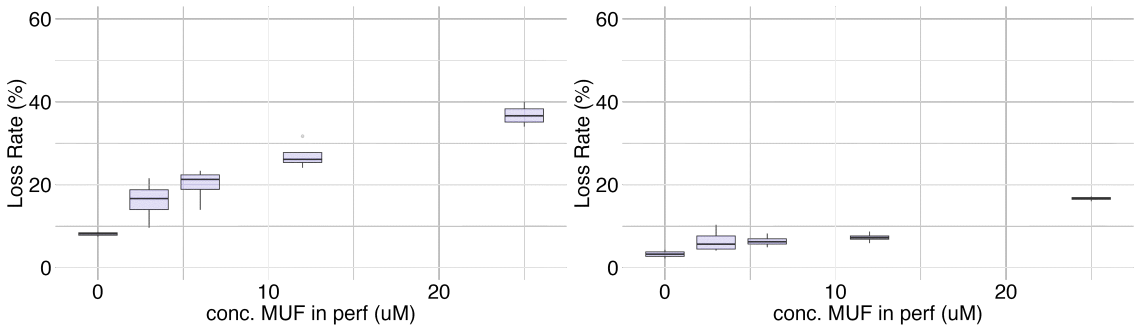

(a) The Loss rate (%)

(b) The Loss rate (%)

Figure 19: The Loss rate (%) depending on the outside concentration with two outside MUF concentration (a) 3.72 μM and (b) 26.13 μM

3.2.2 The MUF-equilibration experiment: calibration

Calibration in experimental part Thinking about the broader picture, the goal of measuring MUF collected in the dialysate is to approximate the enzyme activity rate outside the probe. To do this, we need to estimate the outside MUF concentration that results from enzymatic cleavage, rather than from MUF diffusing out from the perfusate. In this preliminary experiment, using a MUF solution, the objective was to understand the temporal interplay between the outside and inside of the probe, how it affects the MUF collected in the dialysate over time, and to develop a method to correct for the MUF originating from the perfusate.

Examining the data across multiple external MUF concentrations, we can see that the relationship between MUF in the perfusate and MUF in the dialysate was linear at both time points (see Fig. 20). The curves were approximately parallel, shifting upward as the external concentration

increased. For the first 45 min, the slope was 0.271 ± 0.02 SE, and for the second 45 min, it was 0.47 ± 0.01 SE. So the MUF in the dialysate after 45 min can be expressed as:

$$C_{\text{dialysate}} = b + 0.27 \cdot C_{\text{perfusate}} \tag{15}$$

As the lines are parallel and shift upward with increasing external concentration, the only parameter that depends on the external concentration is the y-intercept b. Moreover, the y-intercept b represents the MUF collected in the dialysate when the perfusate contains only water. Thus, having an estimate of the MUF concentration in the dialysate that originates only from enzymatic cleavage (b), b can be used to approximate the external MUF concentration when no MUF is present in the perfusate. In microdialysis measurements, a common approach to estimate the outside concentration is to correct for the recovery rate (Shippenberg and Thompson, 1997). Here, using the recovery rate (RR) determined experimentally by Thayer Taft (see Figure 6) and dividing the collected amount by the sampling duration, we can approximate the MUF production rate as:

$$\text{MUF}^{\text{prod}} \left[\frac{\mu M}{\text{min}}\right] = \frac{b}{RR \cdot t} = \frac{C_{\text{dialysate}} - 0.28 \cdot C_{\text{perfusate}}}{RR \cdot t} \tag{16}$$

where t is the sampling duration in minutes in this case 45. Note that, unlike in the conventional method, the rate of MUF production is not expressed as an absolute amount produced per gram of soil per minute, because both the external volume and the exact mass of soil affected by the method are unknown.

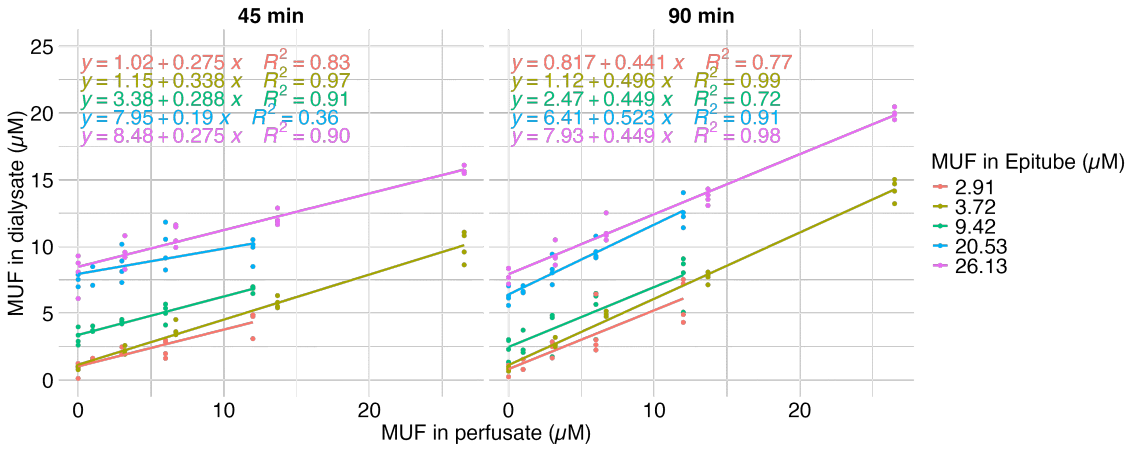

Figure 20: The relationship between the MUF in the perfusate and in the dialysate with five different values of outside MUF concentrations

Calibration in simulation part As we planned to test the calibration in the simulation, we reproduced the MUF equilibration setup of the experiment using different MUF outside-vial con-

centrations and different MUF concentrations in the perfusate, thereby reproducing Fig. 20 after 45 min in the model. This led to Fig. 21 and to the same equation as in the experimental part (see equation 17).

The only striking difference between the simulation and the experimental results is that we recover less. The slope is the same, but the intersection with the y-axis is lower.

$$\mathrm{MUF}^{\mathrm{prod}} \left[\frac{\mu\mathrm{M}}{\mathrm{min}}\right] = \frac{b}{RR \cdot t} = \frac{C_{\mathrm{dialysate}} - 0.28 \cdot C_{\mathrm{perfusate}}}{RR \cdot t} \tag{17}$$

where t is the sampling duration in minutes, in this case 45.

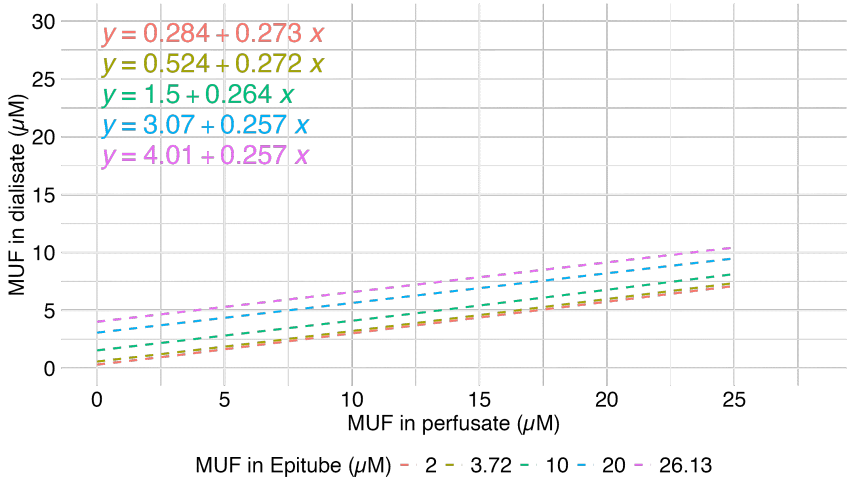

Figure 21: **Simulation** — The relationship between MUF in the perfusate and in the dialysate with five different values of outside MUF concentrations.

Summary In this section, we showed that MUF may adhere to the microdialysis tubing system. Nevertheless, we developed a method to estimate the external MUF concentration arising solely from EEA, effectively removing the background contribution from MUF present in the perfusate. This approach enables us to approximate the extracellular enzyme activity (EEA) outside the probe.

3.3 Michaelis–Menten: Core experiments

3.3.1 Michaelis Menten Microdialysis Enzyme Activity Experiment

In the last section (3.2.2), we introduced a method to correct for MUF in the perfusate and approximate the MUF concentration outside the probe resulting from enzymatic cleavage, thereby estimating the rate of enzymatic activity. The rate of cleavage depends on the substrate (MUF–NAG) concentration and follows a Michaelis–Menten curve. The two key parameters are $v_{\max}$, the maximum turnover rate, and K_m, the Michaelis constant, both of which are essential for quantifying extracellular enzyme activity in soil. In this section, we address the following question:

- Can we reproduce a Michaelis–Menten curve using microdialysis?

Model results Before analyzing the experimental results, we first tested whether the microdialysis method is theoretically suited to measure extracellular enzyme activity (EEA) and whether it can reproduce a Michaelis–Menten relationship in simulation. To this end, we simulated perfusion with five different MUF–NAG concentrations (4000, 2000, 1000, 500, and 250 μM) combined with three different $v_{\max} \cdot [E]$ values. In this simplified setup, the perfusate was assumed to contain only MUF–NAG, without any residual free MUF, allowing us to directly evaluate whether MUF collected via microdialysis would theoretically follow a conventional Michaelis–Menten curve.

The simulation results (Fig. 22a & b) show that the modeled microdialysis indeed produced Michaelis–Menten curves. However, the saturation levels did not correspond to the implemented $[E] \cdot v_{\max}$ values as expected. Instead, they were approximately twice as low. Nevertheless, the differences in MUF^{prod} closely reflected the proportional differences in $v_{\max} \cdot [E]$. Overall, the resulting curves approximated a Michaelis–Menten relationship, supporting the theoretical feasibility of the approach.

We next considered a more realistic scenario in which 0.25% of the total MUF–NAG concentration in the perfusate was present as free MUF. In this setup, free MUF altered the concentration gradient dynamics between the probe interior and the surrounding environment over time. This leads to a different temporal dynamics of the MUF collected (see Fig. 15). Correcting for this contribution is therefore essential, which we addressed by applying the calibration described in Equation 16 to the MUF collected (Fig. 22c c & d). To test its validity, we compared calibrated results to the baseline case without free MUF (Fig. 22a & b), expecting recovery of a Michaelis–Menten relationship.

In the solution setup, the calibration successfully reproduced the baseline dynamics: the overall range of MUF^{prod} and the shape of the saturation curve were nearly identical (Fig. 22a & 22e).

We then tested whether the same calibration applies to soil cores, where the effective diffusion volume is smaller due to reduced radius and porosity. In this case, the calibration preserved the relative differences between enzyme levels and the general range of MUF^{prod}, but failed to yield a clear Michaelis–Menten curve. Saturation was not observed, indicating that diffusion constraints in cores fundamentally alter the kinetics (Fig. 22f).

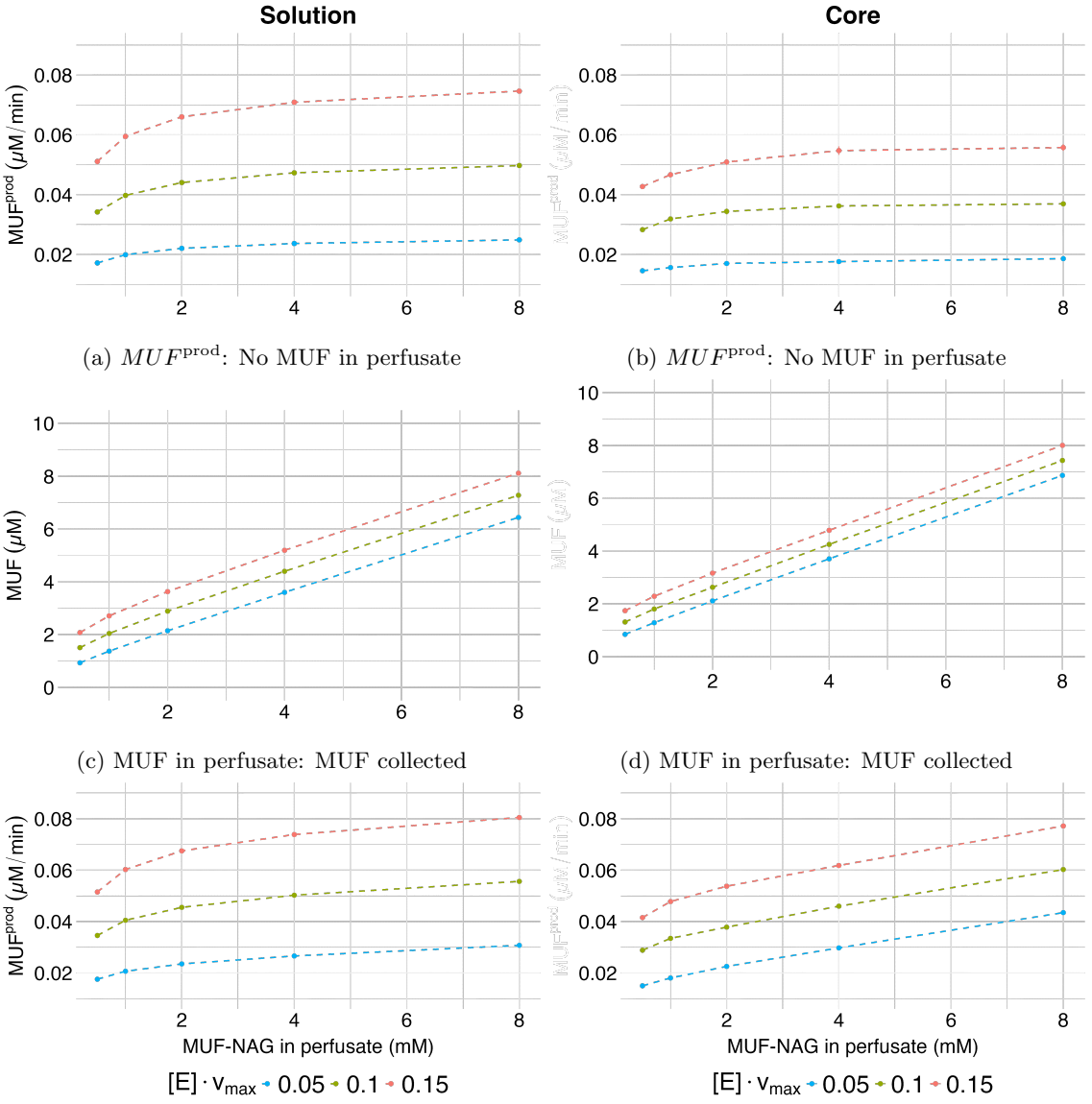

(a) MUF^{prod}: No MUF in perfusate

(b) MUF^{prod}: No MUF in perfusate

(c) MUF in perfusate: MUF collected

(d) MUF in perfusate: MUF collected

(e) MUF in perfusate: Calibrated (solution)

(f) MUF in perfusate: Calibrated (core)

Figure 22: **Simulation** — After 45 minutes of perfusion with varying MUF–NAG concentrations, measurements are compared with simulations using different $v_{\max} \cdot [E]$ values in two volume environments corresponding to soil cores and solution. (a) and (b): MUF^{prod} in simulations in which no MUF is present in the perfusate. (c) and (d): collected MUF (μM). (e) and (f): calibrated MUF^{prod} using the calibration for the model presented in Section 3.2.2.

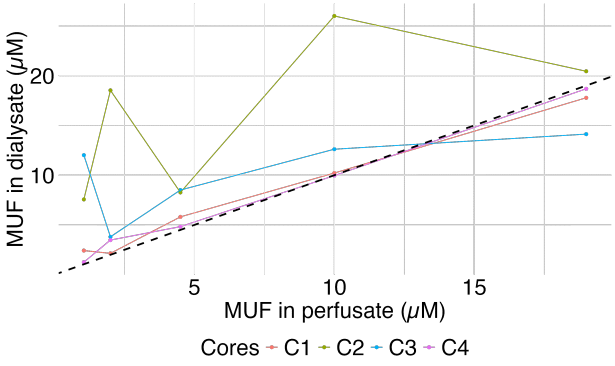

(a) MUF collected (μM)

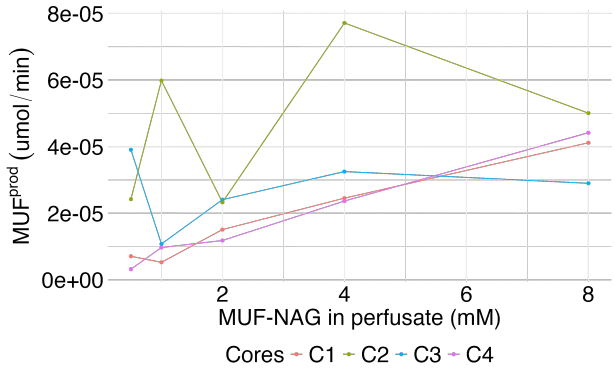

(b) Estimated MUF production using calibration 1 (μmol/min)

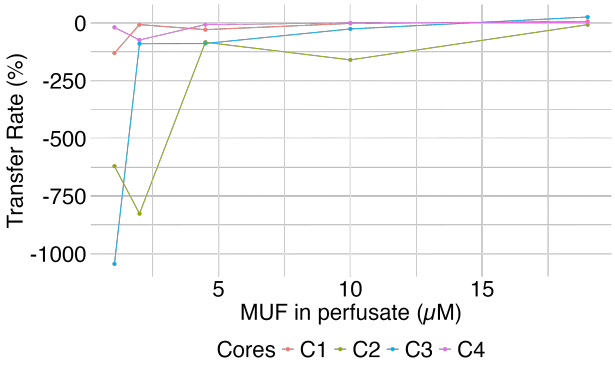

(c) Transfer rate of MUF (%)

Figure 23: Relationship between MUF in the perfusate and in the dialysate after 45 min of perfusion with different MUF–NAG concentrations. The black dashed line represents the identity line, $f(x) = x$. C1, C2, C3, C4 are the 4 core replicates from the same 16m^2 spot in the forest.

Experimental results. Now, we present a reverse microdialysis experiment using soil cores for the first time. As in the previous modeling section, our goal was to determine whether we could reproduce a Michaelis–Menten curve. Four cores were used, all originating from the same 16 m^2 spot in the forest. Over 3 h, five different MUF–NAG concentrations were perfused, and a dialysate was collected every 45 min. Here, we focus only on the results after 45 min (results for other time points are provided in Supplement 4), as this is the time point for which we developed a calibration, enabling us to approximate the MUF cleavage rate (for more details, see Section 3.2.2). The MUF measured in the dialysate was then corrected for residual MUF using the established calibration (Equation 16).

MUF collected in the first dialysate sample (0–45 min) from cores C1 and C4 shows a linear relationship (Fig. 23a), with the resulting curve closely following the identity line (black dashed line in Fig. 23a). By contrast, cores C2 and C3 exhibit no consistent trend, with C2 displaying particularly high variability. MUF concentrations in the dialysate range from 1.25 to 26 μM.

After applying the calibration, the estimated MUF production shows a trend comparable to the collected MUF, but no clear Michaelis–Menten behavior is observed (Fig. 23b).

Transfer rates increase with perfusate concentration, ranging from –1044.15% to 25.65%, and

rapidly approach zero at higher MUF concentrations in the perfusate. The highest MUF concentrations and most extreme transfer rates occur in cores C2 and C3, suggesting the strongest fluxes between soil and probe and thus the highest extracellular enzyme activity (EEA) (Fig. 23c).

Summary Theoretically (in the model), by combining calibration and reverse microdialysis in a solution, it is possible to reproduce a Michaelis–Menten curve. However, we were not able to reproduce the curve either in the simulated soil core or in the experimental setup.

3.4 Final core experiments

3.4.1 The Retrieval Experiment

Before finally performing the experiment to estimate enzyme activity in the soil core with the microdialysis method, it is important to consider an additional challenge. Contrary to the conventional method, which estimates enzyme activity using the wells of a 96-well plate by measuring the MUF cleaved directly in the well, in the case of microdialysis the measured MUF in the dialysate results from the recovered MUF around the probe through diffusion processes between the probe and the surrounding solution. Moreover, in the case of the core, MUF can diffuse away from the probe over time and interact with soil particles. Therefore, we will focus on the question:

- How much of the introduced MUF is actually recoverable?

In the first phase, MUF was introduced into soil cores for either 45 min or 90 min, after which the perfusate was switched to ultrapure water to monitor recovery. In both treatments, switching from MUF-containing perfusate to water (illustrated by the blue horizontal line in Fig. 24) caused a rapid decline in MUF concentration in the dialysate, which then converged to zero.

During the 270 min introduction phase, MUF accumulated around the microdialysis probe, with dialysate concentrations gradually increasing and reaching equilibrium at approximately 135 min, stabilizing at about 75% of the perfusate concentration. In the 45 min introduction phase, 0.000856 µmol of MUF was introduced, of which 0.000699 µmol was recovered. In the 270 min phase, 0.002433 µmol was introduced, with an average of 0.00150 µmol recovered.

Overall, the retrieval rate in the long-introduction treatment was $72.2\% \pm 13.9$ SE, lower than in the short-introduction phase, where it reached $81.9\% \pm 4.5$ SE.

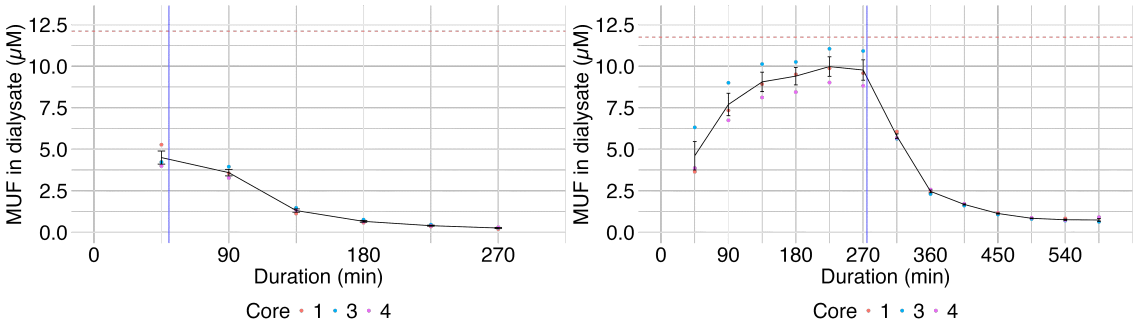

(a) 45 min of introduction

(b) 270 min of introduction

Figure 24: MUF collected in the dialysate overtime (μM). The blue horizontal line indicate the switching form the MUF solution in the perfusate to the water.

3.4.2 Microdialysis Enzyme Activity Experiment

In this final experiment, the goal was to test whether the reverse microdialysis method is sensitive enough to detect changes in extracellular enzyme activity (EEA) induced by pulsed substrate additions. For this purpose, we used soil cores collected from the same 16 m^2 area in the forest, ensuring similar water content and soil structure so that the diffusion volume around the probe was comparable. Every two days over the course of one week, the soil cores were perfused with either water (control), acetate, or NAG. On the final day, exoenzyme activity was measured using the microdialysis-based EEA assay by introducing a substrate solution containing MUF–NAG at a concentration of 4000 μM into all probes, which was then cleaved by the enzymes, and the released MUF was collected. Unlike in the preliminary core experiment, we used a single substrate concentration and compared the amount of MUF collected between treatments, similar to the simulation described in Section 3.1.

The first dialysate, representing the MUF collected between 0 and 45 min, we can calculate the rate of MUF production with the calibration (Eq. 16). The rates ranges from 0.21- 0.38μM $min^{-}1$ and a one-way ANOVA indicated no significant effect of treatment on enzyme activity ($p = 0.149$).

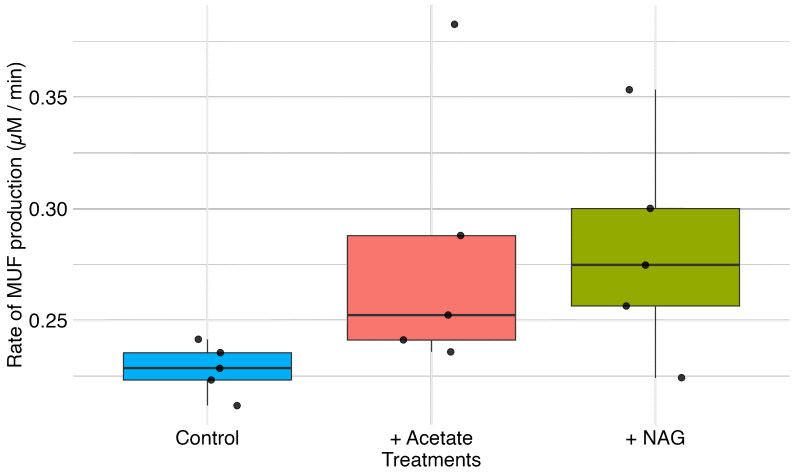

Figure 25: MUF production rates calculated from MUF concentrations collected after 45 minutes and calibrated using Eq. 16. Statistical comparisons were performed using an ANOVA test $p = 0.149$.

To assess the temporal dynamics of MUF flux between the probe and the surrounding soil under different treatments, and to gain insight into EEA over time, we examined the transfer rate (TR). As shown in Section 3.1, simulations indicated that TR can provide valuable information on temporal changes in EEA (see Fig. 17). The transfer rate reflects both the direction and magnitude of flux, with values further from zero representing stronger gradients. Moreover, any value below zero

i.e. when the MUF concentration in the dialysate is higher than in the perfusate, can only result from EEA. The stronger the EEA, the more negative the TR becomes. Across all treatments, transfer rates declined over time (Fig. 26b), ranging from 3.64 to −102%. Rates were consistently higher in the control than in the amended treatments. In both the control and NAG treatments, transfer rates stabilized, whereas in the acetate treatment they continued to decrease. At second and the final three time points, the acetate treatment showed significantly lower transfer rates than the control ($p < 0.01$). The NAG treatment showed intermediate effects: transfer rates did not differ significantly from either the control or the acetate treatment, except at 90 min. Variability was also apparent at the replicate level, with three of the five NAG replicates following the acetate trend, while the remaining two were more similar to the control (Fig. 26c).

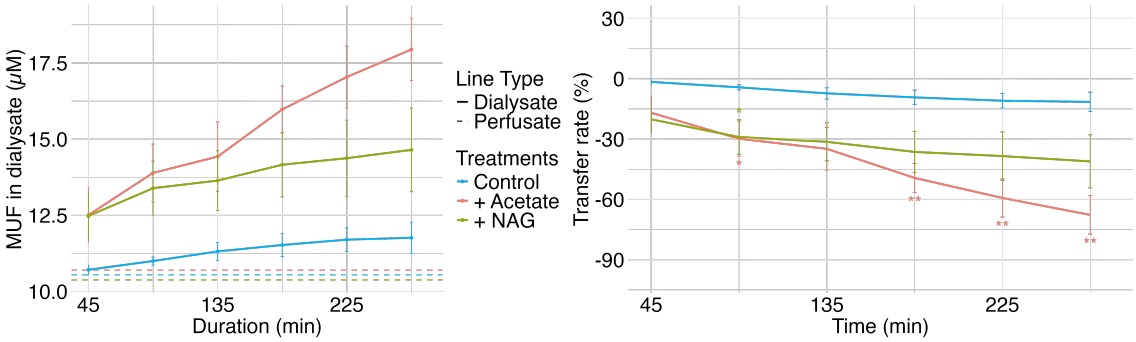

(a) MUF collected (μM)

(b) Transfer rate of MUF

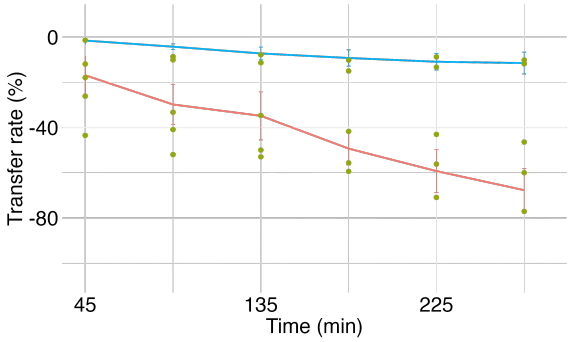

(c) Transfer rate of MUF with +NAG in more detail

Figure 26: Temporal dynamics of MUF collected over the six dialysates in response to a regular pulse (+NAG , + Acetate). Asterisks indicate that the response to substrate significantly differs from the water control using Student's two sample t-test

Summary In this section, we first showed that most of the MUF can be recovered from outside the probe. Moreover, Reverse microdialysis can be used to compare exoenzyme activities following the addition of labile carbon inputs to the same intact soil. In particular, we showed that acetate addition led to an increase in extracellular enzyme activity.

Discussion

The goal of this thesis was to establish reverse microdialysis as a new method for measuring extracellular enzyme activity (EEA) in situ in soil. Microdialysis provides a major advantage by capturing enzyme activity directly in undisturbed soils, offering a more realistic representation of soil processes than conventional methods. In particular, it allows the detection of EEA at a fine spatial scale, rather than averaging across bulk measurements from sieved and ultrasonicated soil slurries, thereby providing more detailed insight into microbial functioning. Furthermore, it excludes contributions from stabilized enzymes bound to organic matter or minerals, which are typically released during sieving and ultrasonication in conventional assays (Buckley et al., 2019; Nannipieri, 2006; Wallenstein and Weintraub, 2008). At the same time, applying reverse microdialysis in soil cores introduces new challenges. In this study, we focused on three of these challenges and explored possible solutions.

How does the system's volume affect the measurement and how much of the introduced MUF can realistically be recovered?

The first challenge of working with soil cores rather than slurries is that the effective system's volume around the probe is unknown and strongly depends on the water content of the soil. Miró et al. (2010) demonstrated that higher soil water content substantially increases solute recovery by microdialysis. More generally, any resistance to diffusion from the surrounding matrix strongly affects recovery rates (Shippenberg and Thompson, 1997). For instance, König et al. (2022) showed that transfer rates into soil are about twofold lower than into Milli-Q water. This reduction may result from the structural complexity of soils, where disconnected water pathways and large aggregates hinder diffusion (König et al., 2022; Nunan et al., 2020; Nunan, 2017; Tecon and Or, 2017).

Model Currently, no method exists to directly measure the system's volume around the probe in soil cores, the space through which substrate (MUF-NAG) and product (MUF) can diffuse. Our model allows us to simulate this system and assess the sensitivity of recovery to two parameters: (i) diffusion radius, which determines the radius of the outer container, and (ii) porosity, which shapes the pore distribution within the soil structure. Incorporating pore structure into the model influences both diffusion pathways and pore accessibility. Together, these parameters define the volume available for diffusion and influence MUF recovery through three mechanisms: larger volumes (i) increase the number of enzymes reached, (ii) delay MUF accumulation to equilibrium,

and (iii) allow more product to diffuse away from the probe. In most cases, higher volume led to increased MUF recovery, indicating that enzyme accessibility (mechanism i) was the dominant factor. This pattern was particularly evident when comparing pore volume to MUF collected (Fig.13). However, when varying diffusion radius between 48 L and 500 L, MUF recovery decreased slightly (Fig.10). This exception relates to accumulation dynamics rather than product loss. System's volume increased equilibration time because accumulation depends on available space (Fig. 8). When MUF begins accumulating near the probe boundary recovery increases temporarily before equilibrating (Fig.9). In total, we have seen that the volume indeed influences the recovery of MUF. However, the model accounts only for diffusion-related losses, not for other processes that may remove MUF from the system, such as abiotic processes like binding to mineral particles in the soil.

Retrieval experiment. In soil cores, when substances are introduced via a semi-permeable membrane, part of the solute may be lost through several processes: (i) diffusing away from the probe, (ii) binding to minerals or being consumed, and (iii) adhering to the dialysis membrane (König et al., 2022; Shippenberg and Thompson, 1997). To estimate how much of the MUF introduced by reverse microdialysis or produced by EEA can maximally be recovered, we performed a pulsing experiment. For this we first introduced a known amount of MUF into the soil, by perfusing it either for a short (45 min) or for a long period (4.5 h). After this, perfusion was switched to water and recovery in the dialysate was tracked. A longer introduction times (simulating longer EEA measuring times), not only increases the total amount of MUF entering the system, but also allows MUF to diffuse further away from the probe and interact longer with soil minerals and microbes. After the short pulse, approximately 82% of the introduced MUF was recovered, while after the long pulse recovery decreased to about 72%. The final dialysate was not fully depleted, suggesting that slightly higher recovery rates might have been reached with a longer waiting period. Nevertheless, these results align with our expectation, that part of the introduced MUF becomes unavailable for recovery due to diffusion losses and interactions in the soil matrix. Nevertheless, the variability of MUF in the dialysate (µM) within cores was very low (0.001–2.20; see Figures 24a 24a), indicating that local differences in soil structure within a single soil over distances of a few meters are negligible.

Sticking to the probe Another factor affecting MUF recovery in the dialysate is adsorption to the microdialysis tubing. Depending on the tubing material and the perfusate composition, molecules can bind to the probe walls, as previously reported for other substances (Nirogi et al.,

2012; Shippenberg and Thompson, 1997).

In the MUF–equilibration experiment 3.2, the observed relationship between MUF in the perfusate, MUF outside the probe, and MUF collected in the dialysate differed from expectations. Notably, when the MUF concentration in the perfusate equals that outside the probe, no net flux should occur over time, this is indicated by the intersection of curves representing two different time points (Fig. 18b). However, this intersection was much lower than expected. Because the microdialysis setup was closed, all MUF not recovered in the dialysate should have been detectable in the surrounding Eppendorf solution, yet 15.56% (±1.74%) of MUF was unaccounted for (Fig. 18b). This suggests that passive diffusion alone cannot explain the observed dynamics and supports the hypothesis that MUF adheres to the tubing surface. Incorporating a sticking term into the model reproduced the observed shift (Fig. 18c), confirming that surface interactions significantly influence solute behavior in this system.

Summary Meaningful comparisons using microdialysis are only possible between soil cores that share similar structure and water content, as both factors strongly influence diffusion and recovery. While the variability of MUF recovery within cores was very low, this indicates that the effect of soil structure over distances of a few meters is negligible. Overall the recovery was substantial, with 72% of the introduced MUF being recovered for the long introduction period, which corresponds to the duration of our final experiment. This indicates that a significant fraction of the solute accumulates in the soil matrix around the probe but can still be retrieved within the experimental timeframe.

Correcting for MUF in the perfusate and testing Michaelis–Menten kinetics

To test whether reverse microdialysis is suitable for measuring extracellular enzyme activity is to see if it can reproduce a Michaelis–Menten curve. We therefore introduced different MUF–NAG concentrations and evaluated whether the measured rate increases at low substrate and saturates at high substrate. This required translating the MUF concentration collected in the dialysate into an enzyme cleavage rate. A key challenge is that the perfusate itself contains free MUF. Because reverse microdialysis depends on time-dependent diffusion, simple subtraction of perfusate MUF from dialysate MUF is invalid: the fraction of dialysate MUF that originates from the perfusate versus enzymatic cleavage changes over time, so the two sources cannot be distinguished by a single baseline correction (see Fig. 15).

The correction we presented in the section 3.2.2, which allows us to estimate the external MUF

concentration as if no MUF were present in the perfusate, is based on the results of the MUF–MUF equilibration experiment (Fig. 20). In this experiment, we found a linear relationship between MUF in the perfusate and in the dialysate. The slope of this relationship after 45 min was independent of the external concentration, while the y-intercept increased with increasing outside concentration. This intercept represents the amount of MUF that would be collected after 45 min of perfusion if the MUF–NAG solution contained no residual MUF. We use this relationship to calibrate MUF concentrations from EEA experiments and to approximate the external MUF concentration in the absence of MUF in the perfusate (see Equation 16).

Model Having established a way to experimentally calibrate MUF concentrations in the dialysate to approximate external MUF concentrations outside the probe, we mirrored the same approach in the NetLogo model (see Section 3.2.2). In the first scenario, no MUF was present in the perfusate, serving as a baseline. In the second, MUF was included in the perfusate, with the surrounding solution replicating the MUF–MUF equilibration experiment (see Fig. 21). In this case, applying the calibration based on the model-derived correction factors allowed the model to recover Michaelis–Menten kinetics, with resulting rates closely matching the baseline scenario (Figs. 22). In the third scenario, the perfusate contained MUF, but the surrounding environment was set to a core with reduced system's volume. This was achieved by decreasing the diffusion radius, $d_{\max}$, and reducing the number of pore cells, mimicking the limited water-filled pathways in soil cores. Under these conditions, the calibration failed to reproduce Michaelis–Menten kinetics. This discrepancy likely arises because the calibration, developed in an open solution with free diffusion, cannot account for the constrained diffusion environment in soil cores. Higher resistance to diffusion and limited surrounding volume are known to significantly affect recovery rates (Shippenberg and Thompson, 1997), and in vitro calibrations have been shown to fail under such constrained conditions (Glick et al., 1994). Beyond these diffusion constraints, real soil cores introduce additional complexity through spatial heterogeneity.

Experimental Data Core 3 displayed large variability in MUF collected, largely independent of perfusate MUF–NAG concentration. This likely reflects heterogeneous enzyme distribution and local differences in water content (Young and Crawford, 2004; Tecon and Or, 2017; Nunan, 2017; Nunan et al., 2020), both of which strongly influence substrate diffusion and probe–soil contact (Burns et al., 2013; Miró et al., 2010). However, Core 3 showed higher calibrated MUF rates, consistent with conventional assays (Fig. 23c 7).

Nevertheless, the calibrated MUF production rate MUF^{prod} did not show saturation with increas-

ing MUF–NAG input. In contrast, Cores 1 and 4 displayed a different pattern: MUF collected was nearly equal to the perfusate concentration, showing a very linear relationship after calibration (Fig. 23c). One reason could be that, as discussed in the model section, the calibration baseline was carried out under different conditions, in a well-mixed, free diffusion, larger volume, than those of the soil cores. Consequently, differences in external volume may have caused the calibration to fail, similar to what was observed in the model-calibrated cores (Fig. 22). Indeed, as seen in section 3.1, volume alters the flux of MUF. Another possibility is that the 45-min perfusion period was too short for sufficient substrate transfer, so the external substrate concentration likely did not reach enzyme saturation.

Summary The calibration appears to be a promising tool for correcting the presence of MUF in the perfusate, as demonstrated in the model solution environment. However, the calibration did not reproduce Michaelis–Menten kinetics in soil cores, either in the model simulation or in the experimental results. Possible reasons include using a baseline under conditions very different from those in the soil cores, or that the 45-min perfusion period may have been too short for sufficient substrate transfer.

Can microdialysis detect significant changes in *in situ* enzyme activity?

In this part, we wanted to check if changes in EEA can be captured using reverse microdialysis within one soil after pulsing different carbon compounds.

Transfer Rate as an Indicator for EEA The concentration gradient between the microdialysis probe and its surrounding medium is the primary driver of solute flux into the dialysate. When concentrations are higher outside the probe, MUF diffuses inward, depleting the external pool and reducing flux. When concentrations are higher inside, diffusion occurs outward. Once equilibration is reached, no net transfer occurs and MUF levels in the dialysate stabilize. Looking at the time series of the transfer rate (TR) thus captures the temporal dynamics of substance accumulation around the probe. The TR, normalized by the perfusate concentration, reflects the direction and magnitude of solute flux relative to the probe but does not directly indicate the absolute concentrations in the surrounding soil. It is influenced not only by the properties of the solute (e.g. molecular weight) but also by the surrounding medium (König et al., 2022). For this reason, soil-specific characteristics must be considered when comparing TR across systems (Buckley et al., 2019). In our study, however, comparisons were made within the same soil type using the same MUF–NAG and MUF concentrations in the perfusate under different treatments, ensuring that

soil structure and water content remained consistent. Retrieval experiments further supported this assumption: variability within a single soil core was minimal, suggesting a comparable effective diffusion volume across probes (Fig. 24b). In this case, the significant differences in TR can only result from differences in external MUF concentrations.

Monitoring transfer rates over time can therefore serve as a proxy for extracellular enzyme activity (EEA) in the surrounding of the probe. Model simulations support this interpretation: within the same environment, TR trajectories diverged with increasing enzyme concentrations (Fig. 17). Higher enzyme activity accelerated MUF–NAG cleavage, leading to elevated external MUF concentrations. As a result, flux reversed sooner and more strongly, producing increasingly negative TR values in proportion to enzyme activity.

Microbial Response to Acetate Addition In our experiment, repeated acetate pulses led to a significantly lower transfer rate in the last three dialysate (Figure 26b), which is an indication for higher enzyme activity. One known effect of adding acetate, a charged organic acid, is the destabilization of organo-mineral bonds, releasing organic compounds that become accessible to microorganisms (Keiluweit et al., 2015; Jilling et al., 2021; Clarholm et al., 2015). This can occur via acidification, chelation, or exchange reactions. Additionally, acetate can act as a direct carbon source for microorganisms (Wiesenbauer et al., 2024a). This shift from carbon limitation to availability may activate dormant microbes, promote microbial growth, and stimulate enzyme production (Mondini et al., 2006; Kuzyakov and Blagodatskaya, 2015).

The different responses to the NAG pulses The effects of N-acetylglucosamine (NAG) on extracellular enzyme activity (EEA) are complex and less straightforward. NAG can act as a signaling molecule indicating the presence of substrate, serve as a nutrient source, or function as a downregulating signal when nutrient scarcity is alleviated (Allison et al., 2011; Chróst, 1991; Allison and Vitousek, 2005; Schimel and Weintraub, 2003). Which mechanism dominates likely depends on local NAG concentrations and the specific responses of microbial communities (Allison and Vitousek, 2005; Carreiro et al., 2000).

As shown in Figure 26c, following NAG pulses, two replicates behaved similarly to the control, while three resembled the response observed with acetate addition. One possible explanation is spatial heterogeneity in nutrient availability. In microsites already containing similar NAG concentrations, no additional response may occur because NAG does not act as a signal. By contrast, in microsites where NAG or other nitrogen sources are scarce, an elevated concentration may signal the presence of substrate, leading microbes to increase enzyme production. In some communities, however, the

presence of NAG may downregulate enzyme production, as the need for polymer degradation is reduced.

Another explanation is that NAG may function as both a carbon and nitrogen source, thereby supporting microbial growth in a manner similar to acetate. The variability in response could then reflect differences in community composition: NAG uptake requires specific transport systems, which are not universally present, meaning only specialized microbial groups can use NAG as both carbon and nitrogen (Riemann and Azam, 2002).

Summary Our results demonstrate that reverse microdialysis, combined with transfer rate analysis, can capture temporal differences in extracellular enzyme activity within a given soil.

Conclusion & Outlook

Using reverse microdialysis in combination with analysis of the temporal dynamics of the transfer rate provides valuable insights into different exoenzyme activity responses following the addition of labile carbon inputs to the same intact soil. This approach opens new opportunities for understanding soil processes in their natural environment, such as enzymatic responses to events like root exudation. A promising direction for future research is to explore microbial regulatory mechanisms in response to varying product levels. For example, extending the analysis to a broader range of NAG concentrations and examining the resulting responses. This could be combined with analyzing solutes collected during the initial pulse phase, which could help explain observed differences between treatments.

While analyzing the temporal dynamics is effective for comparing treatments that do not alter soil structure, using the transfer rate alone does not provide a direct measure of enzymatic cleavage rates as conventional enzyme assays do. In this thesis, a calibration was developed to link the MUF collected to an approximation of the production rate outside the probe. Although the calibration failed to reproduce Michaelis–Menten kinetics in soil cores, it highlights a critical constraint: calibration must be performed under the same diffusible volume as the measurement. To address this, future work could develop calibration curves in a smaller external volume, closer to the water content near the probe, or perform a calibration experiment immediately before the treatment experiments using the same soil. Developing a calibration applicable within the same core could also enable comparisons across different soil types.

Validation of the calibration could be achieved by replicating an external enzymatic activity setup similar to the calibration solution. Microdialysis experiments in an aqueous solution containing a

known enzyme concentration would minimize spatial heterogeneity, allowing for clearer assessment of Michaelis–Menten kinetics and more robust validation of the calibration model.

In summary, for experiments within a single soil where structure is not altered, analyzing temporal dynamics of the transfer rate is a robust approach to compare exoenzyme activity. If the objective is to quantify production rates outside the probe, microdialysis remains a promising tool but requires further calibration development to achieve accurate and comparable measurements across different soils.

Supplements

Result Supplement

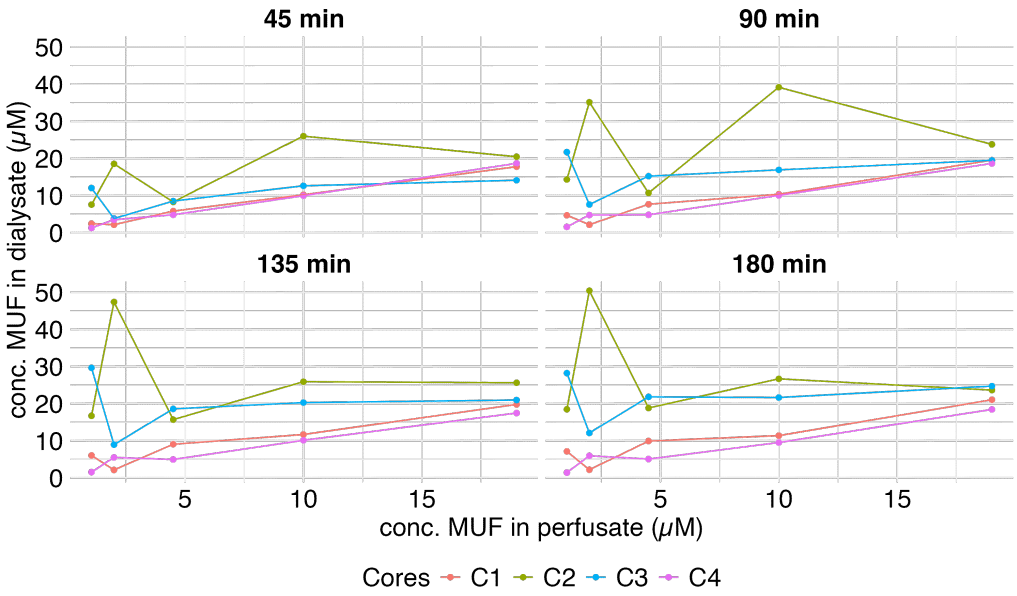

Figure 27: The relationship between MUF in the perfusate and in the dialysate in the four dialysates, when perfusing different MUF-NAG ($8000, 4000, 2000, 1000$ and 500 μM) concentrations

Model Supplement

Testing Two Different Grid Sizes

In the model, we discretize continuous phenomena in both time and space. Spatial discretization introduces an error that is proportional to the cell size, Δx. In this section, we compare two different cell sizes: $\Delta x = 0.2$ mm and $\Delta x = 0.46$ mm, the second one being the size used in our main simulations, to evaluate whether the chosen Δx is acceptable.

Table 2 summarizes how key parameters change with the grid size:

Symbol	$\Delta x = 0.2$	$\Delta x = 0.46$	Units
Δd	0.4	0.46	mm
Δx^3	0.016	0.097	μL
Δt	10	10	s
L_t	1.02	1.012	cm
h_t	0.4	0.46	cm
u	2.46	2.46	μL / min
RR	73	72.5	%
TR^*	11.5	14.5	%

Table 2: Values used in the model for the two different grid sizes. * The transfer rate was calculated with $10\mu M$ in the perfusate and nothing outside after 45 min of perfusion

Since diffusion is discretized in space, the choice of Δx influences both the transfer and recovery rates, although the resulting differences remain small (see Table 2).

Kurzfassung

Bodenmikroorganismen produzieren extrazelluläre Enzyme, die pflanzliche und mikrobielle organische Substanzen depolymerisieren und dadurch Produkte freisetzen, die sie assimilieren können. Diese Enzyme haben einen entscheidenden Einfluss darauf, ob und in welchem Tempo organische Substanzen im Boden zersetzt oder stabilisiert werden. Da der Boden eine hochkomplexe und heterogene Umgebung darstellt, kann die Exoenzymaktivität auf sehr kleinen räumlichen Skalen variieren, manchmal nur über wenige Millimeter hinweg. Die Aktivitätsniveaus hängen von mehreren Faktoren ab, wie etwa der Nährstoffverfügbarkeit und der Substratqualität, und spiegeln die mikrobielle Regulation der Enzymproduktion wider. In-situ-Messungen ermöglichen es, die räumliche und zeitliche Dynamik der mikrobiellen Enzymaktivität zu erfassen.

Die *reverse Microdialysis* ist ein minimal-invasives Verfahren zur kontinuierlichen Gewinnung und Einführung frei diffusibler, wasserlöslicher Substanzen aus der Umgebung entlang eines Konzentrationsgradienten. Durch die Anwendung der Mikrodialyse in intakten Bodenproben können Substrate eingebracht und Reaktionsprodukte gewonnen werden, ohne den umgebenden Boden wesentlich zu stören. Hier wird ein neuer In-situ-Ansatz zur Messung der Enzymaktivität im Boden vorgestellt, bei dem ein fluoreszierendes Substrat, 4-Methylumbelliferyl-N-acetyl-β-D-glucosaminid (MUF–NAG), verwendet wird. Dieses wird in den Boden eingebracht und anschließend enzymatisch gespalten, sodass das fluoreszierende Produkt (MUF) mittels Mikrodialyse entnommen werden kann. Parallel zu den Experimenten wurde ein Modell entwickelt, um die Mikrodialyse-Sonde und die damit verbundenen Stoffflüsse zu simulieren.

Im Gegensatz zu herkömmlichen Bodenenzymtests und Modellsimulationen reproduzierte die Mikrodialyse nicht die typische Michaelis-Menten-Kinetik. Jedoch wurde eine neue Kalibrierungsmethode entwickelt, die eine Abschätzung der Enzymproduktionsraten unter In-situ-Bedingungen ermöglicht. In einem zweiten Experiment wurde gezeigt, dass die Zugabe von Acetat, einer labilen Kohlenstoffquelle, die Exoenzymaktivität im Vergleich zur Kontrolle erhöhte. Im Gegensatz dazu hatte

die Zugabe von N-Acetylglucosamin (NAG), einem Produkt der enzymatischen Spaltung, eine variablere Wirkung.

Zusammenfassend wird gezeigt, dass die umgekehrte Mikrodialyse verwendet werden kann, um Exoenzymaktivitäten nach der Zugabe von labilen Kohlenstoffquellen in demselben intakten Boden zu vergleichen. Dieser Ansatz kann Einblicke in enzymatische Reaktionen auf Ereignisse wie Wurzelausscheidungen liefern. In dieser Studie führte die Zugabe von Acetat zu einer erhöhten extrazellulären Enzymaktivität, möglicherweise infolge der Freisetzung gebundener Mineralstoffe durch Ionenaustauschprozesse. Die Assimilation dieser freigesetzten Nährstoffe oder des Acetats selbst durch Mikroorganismen kann das Wachstum stimulieren oder ruhende Zellen aktivieren und dadurch die Enzymaktivität verstärken.

Summary

Soil microorganisms secrete extracellular enzymes that depolymerize plant- and microbe-derived organic matter, producing compounds they can assimilate. These enzymes strongly influence whether soil organic matter is decomposed or stabilized, and at what rate. As soil is a highly complex and heterogeneous environment, exoenzyme activity can vary at very small spatial scales, sometimes just millimeters apart. Activity levels depend on multiple factors, such as nutrient availability and substrate quality, and reflect microbial regulation of exoenzyme production. Therefore, in situ measurements are essential to capture the spatial and temporal dynamics of microbial enzyme activity.

Reverse microdialysis is a passive method that enables the introduction and collection of low-molecular-weight compounds based on concentration gradients. By applying microdialysis tubing in intact soil cores, substrates can be introduced and reaction products can be recovered with minimal disturbance to the surrounding soil. Here, a new in situ approach is presented for measuring enzyme activity in soil, using the fluorescent substrate 4-Methylumbelliferyl N-acetyl-β-D-glucosaminide (MUF-NAG), which is introduced into the soil and then enzymatically cleaved, allowing the fluorescent product (MUF) to be sampled via microdialysis. In addition to the experimental work, a model has been developed to simulate the microdialysis probe and the associated fluxes.

Unlike conventional soil enzyme assays and model simulations, microdialysis did not reproduce typical Michaelis–Menten kinetics. However, I introduce a new calibration method that enables estimation of enzyme production rates under in situ conditions. In a second experiment, I show that introducing acetate, a labile carbon source, increased exoenzyme activity relative to the control. In contrast, pulsing N-acetylglucosamine (NAG), a product of enzymatic cleavage, had a more variable effect.

In conclusion, I demonstrate that reverse microdialysis can be used to compare exoenzyme activities

following the addition of labile carbon inputs to the same intact soil. This approach could provide insight into enzymatic responses to events such as root exudation. In this study, acetate addition led to increased extracellular enzyme activity, potentially due to the release of bound mineral nutrients through mineral exchange. The assimilation of these released nutrients, or of the acetate itself, by microorganisms may stimulate growth or activate dormant cells, thereby enhancing enzyme activity.

Bibliography

Steven D Allison. Cheaters, diffusion and nutrients constrain decomposition by microbial enzymes in spatially structured environments. *Ecology Letters*, 8(6):626–635, 2005.

Steven D Allison and Peter M Vitousek. Responses of extracellular enzymes to simple and complex nutrient inputs. *Soil Biology and Biochemistry*, 37(5):937–944, 2005.

Steven D Allison, Tracy B Gartner, Keri Holland, Michael Weintraub, and Robert L Sinsabaugh. Soil enzymes: linking proteomics and ecological processes. *Manual of environmental microbiology*, pages 704–711, 2007.

Steven D Allison, Michael N Weintraub, Tracy B Gartner, and Mark P Waldrop. Evolutionary-economic principles as regulators of soil enzyme production and ecosystem function. *Soil enzymology*, pages 229–243, 2011.

Gaël Alvarez, Tanvir Shahzad, Laurence Andanson, Michael Bahn, Matthew D Wallenstein, and Sébastien Fontaine. Catalytic power of enzymes decreases with temperature: New insights for understanding soil c cycling and microbial ecology under warming. *Global Change Biology*, 24 (9):4238–4250, 2018.

Dayakar V Badri and Jorge M Vivanco. Regulation and function of root exudates. *Plant, cell & environment*, 32(6):666–681, 2009.

Scott Buckley, Diane Allen, Richard Brackin, Sandra Jämtgård, Torgny Näsholm, and Susanne Schmidt. Microdialysis as an in situ technique for sampling soil enzymes. *Soil Biology and Biochemistry*, 135:20–27, 2019.

Peter M Bungay, Paul F Morrison, and Robert L Dedrick. Steady-state theory for quantitative microdialysis of solutes and water in vivo and in vitro. *Life sciences*, 46(2):105–119, 1990.

Richard G Burns. Enzyme activity in soil: location and a possible role in microbial ecology. *Soil biology and biochemistry*, 14(5):423–427, 1982.

Richard G Burns, Jared L DeForest, Jürgen Marxsen, Robert L Sinsabaugh, Mary E Stromberger, Matthew D Wallenstein, Michael N Weintraub, and Annamaria Zoppini. Soil enzymes in a changing environment: current knowledge and future directions. *Soil Biology and Biochemistry*, 58:216–234, 2013.

Alberto Canarini, Christina Kaiser, Andrew Merchant, Andreas Richter, and Wolfgang Wanek. Root exudation of primary metabolites: mechanisms and their roles in plant responses to environmental stimuli. *Frontiers in plant science*, 10:157, 2019.

MM Carreiro, RL Sinsabaugh, DA Repert, and DF Parkhurst. Microbial enzyme shifts explain litter decay responses to simulated nitrogen deposition. *Ecology*, 81(9):2359–2365, 2000.

Ryszard J Chróst. Environmental control of the synthesis and activity of aquatic microbial ectoenzymes. In *Microbial enzymes in aquatic environments*, pages 29–59. Springer, 1991.

Marianne Clarholm, Ulf Skyllberg, and Anna Rosling. Organic acid induced release of nutrients from metal-stabilized soil organic matter–the unbutton model. *Soil Biology and Biochemistry*, 84:168–176, 2015.

Peter M Cox, Richard A Betts, Chris D Jones, Steven A Spall, and Ian J Totterdell. Acceleration of global warming due to carbon-cycle feedbacks in a coupled climate model. *Nature*, 408(6809): 184–187, 2000.

Warren A Dick. Kinetics of soil enzyme reactions. *Methods of soil enzymology*, 9:57–69, 2011.

Hervé Douville, Krishnan Raghavan, James Renwick, Richard P Allan, Paola A Arias, Mathew Barlow, Ruth Cerezo-Mota, Annalisa Cherchi, ThianY Gan, Joëlle Gergis, et al. Water cycle changes. 2021.

Robert Evans, Guilherme Dal Poggetto, Mathias Nilsson, and Gareth A Morris. Improving the interpretation of small molecule diffusion coefficients. *Analytical chemistry*, 90(6):3987–3994, 2018.

Mariela Garcia Arredondo, Yilin Fang, Morris Jones, Steve Yabusaki, Zoe Cardon, and Marco Keiluweit. Resolving dynamic mineral-organic interactions in the rhizosphere by combining in-situ microsensors with plant-soil reactive transport modeling. *Soil Biology and Biochemistry*, 184:109097, 2023. ISSN 0038-0717. doi: https://doi.org/10.1016/j.soilbio.2023.109097. URL `https://www.sciencedirect.com/science/article/pii/S0038071723001591`.

Mark O Gessner, Christopher M Swan, Christian K Dang, Brendan G McKie, Richard D Bardgett, Diana H Wall, and Stephan Hättenschwiler. Diversity meets decomposition. *Trends in ecology & evolution*, 25(6):372–380, 2010.

SD Glick, N Dong, RW Keller Jr, and JN Carlson. Estimating extracellular concentrations of dopamine and 3, 4-dihydroxyphenylacetic acid in nucleus accumbens and striatum using microdialysis: relationships between in vitro and in vivo recoveries. *Journal of neurochemistry*, 62(5): 2017–2021, 1994.

Graham W Gooday. Physiology of microbial degradation of chitin and chitosan. *Biodegradation*, 1:177–190, 1990.

Paige Hansen, Yao Zhang, Ksenia Guseva, Christina Kaiser, and M Francesca Cotrufo. Microbial community regulation of extracellular enzyme production can mediate patterns of particulate and mineral-associated organic matter accumulation in undersaturated soils. *bioRxiv*, pages 2025–07, 2025.

Daniel L Hernández and Sarah E Hobbie. The effects of substrate composition, quantity, and diversity on microbial activity. *Plant and Soil*, 335:397–411, 2010.

Intergovernmental Panel on Climate Change (IPCC). *Summary for Policymakers*, pages 1–24. Cambridge University Press, 2022.

Robert B Jackson, Kate Lajtha, Susan E Crow, Gustaf Hugelius, Marc G Kramer, and Gervasio Piñeiro. The ecology of soil carbon: pools, vulnerabilities, and biotic and abiotic controls. *Annual review of ecology, evolution, and systematics*, 48(1):419–445, 2017.

Andrea Jilling, Marco Keiluweit, Jessica LM Gutknecht, and A Stuart Grandy. Priming mechanisms providing plants and microbes access to mineral-associated organic matter. *Soil Biology and Biochemistry*, 158:108265, 2021.

MJ Kadhim and M Ibraheem Gamaj. Estimation of the diffusion coefficient and hydrodynamic radius (stokes radius) for inorganic ions in solution depending on molar conductivity as electroanalytical technique-a review. *J. Chem. Rev*, 2(3):182–188, 2020.

Marco Keiluweit, Jeremy J Bougoure, Peter S Nico, Jennifer Pett-Ridge, Peter K Weber, and Markus Kleber. Mineral protection of soil carbon counteracted by root exudates. *Nature Climate Change*, 5(6):588–595, 2015.

Ingrid Kögel-Knabner. The macromolecular organic composition of plant and microbial residues as inputs to soil organic matter. *Soil biology and biochemistry*, 34(2):139–162, 2002.

Alexander König, Julia Wiesenbauer, Stefan Gorka, Lilian Marchand, Barbara Kitzler, Erich Inselsbacher, and Christina Kaiser. Reverse microdialysis: A window into root exudation hotspots. *Soil Biology and Biochemistry*, 174:108829, 2022.

Robert J Kremer. Determination of soil phosphatase activity using a microplate method. *Communications in soil science and plant analysis*, 25(3-4):319–325, 1994.

Yakov Kuzyakov. Factors affecting rhizosphere priming effects. *Journal of Plant Nutrition and Soil Science*, 165(4):382–396, 2002.

Yakov Kuzyakov. Priming effects: Interactions between living and dead organic matter. *Soil Biology and Biochemistry*, 42(9):1363–1371, 2010. ISSN 0038-0717. doi: https://doi.org/10.1016/j.soilbio.2010.04.003. URL `https://www.sciencedirect.com/science/article/pii/S0038071710001355`.

Yakov Kuzyakov and Evgenia Blagodatskaya. Microbial hotspots and hot moments in soil: concept & review. *Soil Biology and Biochemistry*, 83:184–199, 2015.

Alejandro G Marangoni. *Enzyme kinetics: a modern approach*. John Wiley & Sons, 2003.

Manuel Miró and Wolfgang Frenzel. The potential of microdialysis as an automatic sample-processing technique for environmental research. *TrAC Trends in Analytical Chemistry*, 24 (4):324–333, 2005.

Manuel Miró, Walter J Fitz, Siegfried Swoboda, and Walter W Wenzel. In-situ sampling of soil pore water: evaluation of linear-type microdialysis probes and suction cups at varied moisture contents. *Environmental Chemistry*, 7(1):123–131, 2010.

P Moldrup, T Olesen, T Komatsu, S Yoshikawa, Per Schjønning, and DE Rolston. Modeling diffusion and reaction in soils: X. a unifying model for solute and gas diffusivity in unsaturated soil. *Soil Science*, 168(5):321–337, 2003.

Claudio Mondini, María Luz Cayuela, MA Sanchez-Monedero, Asunción Roig, and PC Brookes. Soil microbial biomass activation by trace amounts of readily available substrate. *Biology and Fertility of Soils*, 42:542–549, 2006.

Paolo Nannipieri. Role of stabilised enzymes in microbial ecology and enzyme extraction from soil with potential applications in soil proteomics. In *Nucleic acids and proteins in soil*, pages 75–94. Springer, 2006.

NASA. Carbon dioxide – earth indicator, 2025. URL https://science.nasa.gov/earth/explore/earth-indicators/carbon-dioxide/. Accessed: 2025-11-13.

Ramakrishna Nirogi, Vishwottam Kandikere, Gopinadh Bhyrapuneni, Vijay Benade, Ramanatha Saralaya, Shantaveer Irappanavar, Nageswararao Muddana, and Devender Reddy Ajjala. Approach to reduce the non-specific binding in microdialysis. *Journal of neuroscience methods*, 209 (2):379–387, 2012.

Naoise Nunan. The microbial habitat in soil: Scale, heterogeneity and functional consequences. *Journal of Plant Nutrition and Soil Science*, 180(4):425–429, 2017.

Naoise Nunan, Hannes Schmidt, and Xavier Raynaud. The ecology of heterogeneity: soil bacterial communities and c dynamics. *Philosophical Transactions of the Royal Society B*, 375(1798): 20190249, 2020.

Lydia P Olander and Peter M Vitousek. Regulation of soil phosphatase and chitinase activityby n and p availability. *Biogeochemistry*, 49:175–191, 2000.

Johanna Pausch and Yakov Kuzyakov. Photoassimilate allocation and dynamics of hotspots in roots visualized by 14c phosphor imaging. *Journal of Plant Nutrition and Soil Science*, 174(1): 12–19, 2011.

Richard P Phillips, Adrien C Finzi, and Emily S Bernhardt. Enhanced root exudation induces microbial feedbacks to n cycling in a pine forest under long-term co2 fumigation. *Ecology letters*, 14(2):187–194, 2011.

Lasse Riemann and Farooq Azam. Widespread n-acetyl-d-glucosamine uptake among pelagic marine bacteria and its ecological implications. *Applied and environmental microbiology*, 68(11): 5554–5562, 2002.

KR Saiya-Cork, RL Sinsabaugh, and DR Zak. The effects of long term nitrogen deposition on extracellular enzyme activity in an acer saccharum forest soil. *Soil Biology and Biochemistry*, 34(9):1309–1315, 2002.

Joshua P Schimel and Michael N Weintraub. The implications of exoenzyme activity on microbial carbon and nitrogen limitation in soil: a theoretical model. *Soil Biology and Biochemistry*, 35 (4):549–563, 2003.

Steffen Schlüter, Stephane Sammartino, and John Koestel. Exploring the relationship between soil structure and soil functions via pore-scale imaging, 2020.

Toni S Shippenberg and Alexis C Thompson. Overview of microdialysis. *Current protocols in neuroscience*, (1):7–1, 1997.

Madeleine M Stone, Marissa S Weiss, Christine L Goodale, Mary Beth Adams, Ivan J Fernandez, Donovan P German, and Steven D Allison. Temperature sensitivity of soil enzyme kinetics under n-fertilization in two temperate forests. *Global Change Biology*, 18(3):1173–1184, 2012.

Robin Tecon and Dani Or. Biophysical processes supporting the diversity of microbial life in soil. *FEMS microbiology reviews*, 41(5):599–623, 2017.

César Terrer, Sara Vicca, Benjamin D Stocker, Bruce A Hungate, Richard P Phillips, Peter B Reich, Adrien C Finzi, and I Colin Prentice. Ecosystem responses to elevated co 2 governed by plant–soil interactions and the cost of nitrogen acquisition. *New phytologist*, 217(2):507–522, 2018.

Deepali Thakur, Aarti Bairwa, Bhawna Dipta, Prakriti Jhilta, and Anjali Chauhan. An overview of fungal chitinases and their potential applications. *Protoplasma*, 260(4):1031–1046, 2023.

Matthew D Wallenstein and Michael N Weintraub. Emerging tools for measuring and modeling the in situ activity of soil extracellular enzymes. *Soil Biology and Biochemistry*, 40(9):2098–2106, 2008.

Julia Wiesenbauer, Stefan Gorka, Kian Jenab, Raphael Schuster, Naresh Kumar, Cornelia Rottensteiner, Alexander Koenig, Stephan Kraemer, Erich Inselsbacher, and Christina Kaiser. Soil microbes prefer organic acids over sugars in simulated root exudation. *bioRxiv*, pages 2024–12, 2024a.

Julia Wiesenbauer, Alexander König, Stefan Gorka, Lilian Marchand, Naoise Nunan, Barbara Kitzler, Erich Inselsbacher, and Christina Kaiser. A pulse of simulated root exudation alters the composition and temporal dynamics of microbial metabolites in its immediate vicinity. *Soil Biology and Biochemistry*, 189:109259, 2024b.

Uri Wilensky. *NetLogo*. Center for Connected Learning and Computer-Based Modeling, Northwestern University, Evanston, IL, 1999. URL `http://ccl.northwestern.edu/netlogo/`.

Iain M Young and John W Crawford. Interactions and self-organization in the soil-microbe complex. *Science*, 304(5677):1634–1637, 2004.

Lin Zhang, Yi Peng, Jiachao Zhou, Timothy S George, and Gu Feng. Addition of fructose to the maize hyphosphere increases phosphatase activity by changing bacterial community structure. *Soil Biology and Biochemistry*, 142:107724, 2020.